

Dear Professor Joshua Fu:

Here we submit our revised manuscript for consideration to be published on **Atmospheric Chemistry and Physics**

The further information about our manuscript is as follows:

Topic: The wet deposition of the inorganic ions in the 320 cities across China: spatiotemporal variation, source apportionment, and dominant factors

Type of Manuscript: article

Authors: Rui Li^a, Lulu Cui^a, Yilong Zhao^a, Ziyu Zhang^a, Tianming Sun^a, Junlin Li^a, Wenhui Zhou^a, Ya Meng^a, Kan Huang^a, Hongbo Fu^{a,b,c}*

***Corresponding author:**

Hongbo Fu; Address: Department of Environmental Science and Engineering, Fudan University, Shanghai 200433, China; Tel.: (+86)21-5566-5189; Fax: (+86)21-6564-2080; Email: fuhb@fudan.edu.cn

Firstly, we acknowledge the suggestions of editor and anonymous reviewers, and are also grateful to your efficient serving. We have updated the manuscript on the basis of these valuable comments. Our responses were listed as following:

Reviewer #1:

Deposition of inorganic ions is an important indicator of air pollutant emissions and has potentially large impact on ecosystem. Attributed to its large size and complicated sources of atmospheric components, China is of big diversity on inorganic ion deposition and it is great challenge to quantify the spatial and temporal patterns of deposition. Based on intensive sampling and chemical analysis at sites across the country, this work presents informative results on wet deposition of ions, and analyzed the seasonal and annual changes in deposition. The sources of the deposition were evaluated as well based on specific statistic or arithmetic methods. In general, the paper is of comprehensive information and well organized. Before it can be accepted for publication, however, some issues should be further stressed or discussed, and certain information needs to be clarified as well. Details follow.

Comment 1: Section 2.1: sampling site. One of the most valuable contributions of this work is the sampling and chemical analysis at a great number of cities and sites across the country. However, the strategy of the site selection is unclear. How many sites are located in urban and how many are

in remote/suburban regions? Such kind of information is helpful for audience to judge the representativeness of the sampling.

Response: Thank for reviewer's suggestion. (Line 151-152) Indeed, the information about the sampling sites is helpful for reader. Therefore, we have added the detailed description about the sampling sites. The strategy of the site selection is to assure that the monitoring sites in each city were a mixture of urban sites and suburban/rural sites, which can accurately reflect the acid deposition status of each city. In the present study, 850 monitoring sites were located in urban areas and 432 sites were distributed on the rural regions.

Comment 2: Section 2.2: Regarding the sampling, it is unclear whether the sampling covers the whole studying period for all of the sites? Or the sampling period varied by site? If so, what's the reason? Moreover, the frequency of sampling collection should also be described.

Response: Thank for reviewer's suggestion. (Line 159-162) All of the samples were collected in all of the monitoring sites simultaneously. Sampling collection frequency was strongly dependent on the rain event, and each sample was properly collected during the precipitation event when the wet-only deposition instrument was under the normal condition.

Comment 3: Section 2.5, what's the purpose of this section? Was the method applied for the spatial pattern of wet deposition? Is it related with the spatial interpolation? The method should be explained more carefully.

Response: Thank for reviewer's suggestion. (Section 2.5) The GWR model was not related with the spatial interpolation, but reflected the spatial correlation of socioeconomic factors and inorganic ion depositions. The model was to explore the effects of socioeconomic factors on wet deposition of inorganic ions in consideration of the spatial correlation. Compared with the traditional multiple regression analysis, GWR incorporated the spatial weight matrix into the novel model because the inorganic ion deposition fluxes for neighboring cities generally showed the significantly spatial correlation. Furthermore, GWR model can investigate the spatial variability of the correlation between socioeconomic factors and inorganic ion deposition fluxes compared with the multiple regression analysis.

Comment 4: Lines 285-294, Section 3.1, the author stated the decreasing trend of SO₂ and NO_x emissions resulting in the increased pH for the studying period. In Section 3.2, they presented that the peak sulfate and nitrate peaked in 2014, which seems contradicting to the inter-annual variation

of SO₂ and NO_x emissions. Could you explain the possible reasons?

Response: Thank for reviewer's suggestion. (Line 272-305) Indeed, we stressed that the SO₂ and NO_x emissions in most regions of China displayed the decrease during 2011-2016 compared with those before 2000, which led to the higher pH value compared with those before 2000. The result was drawn based on the data comparison with previous studies. However, it did not mean the pH value over China exhibited the linear increase during 2011-2016. Actually, the pH value increased from 2011 to 2014, while it decreased from the peak to the lower value in 2016. Meanwhile, both of the sulfate and nitrate displayed the similarly annual variations with the pH value. It might be attributed to that these acidic ions might be not very sensitive to the emission decrease. Therefore, it was not contradictory.

Comment 5: Lines 383-385. This statement might not necessarily true for China, as coal burning and some industrial sources are also very important sources of NO_x. Vehicle cannot dominate the growth of NO_x emissions and thereby NO₃⁻ concentrations in precipitation. Moreover, what do you mean by "linearly increase"?

Response: I agree with reviewer's suggestion. (Line 390-393) Indeed, the vehicle cannot dominate the growth of NO_x emission. Based on the reference review, we found that the annual trend of nitrate in the precipitation was in good agreement with the ambient NO₂ level. It suggested that stricter controls on NO_x emissions from power plants might be counteracted by the increase of power plants and energy consumption (Liu et al. 2015a; Wang et al. 2018). "Linearly increase" meant that the vehicle emissions displayed the gradual increase since 1998 and the trend was similar to the straight line. It reflected that the NO_x emission from vehicle exhaust exhibited the rapid increase during the past decades. Although the increase of vehicle volume played an important role on the nitrate in the precipitation, the increase of power plants and energy consumption might be more important.

Comment 6: Section 3.2.2. The seasonal variation of sulfate and nitrate concentrations in precipitation could also be influenced by some other factors. For example, if high temperature in summer elevated oxidation of precursors, how could it result in smaller concentrations? Is it possible that more abundant rainfall dilute the concentrations? Moreover, heating in south China is not as frequent as in north. Here I suggest the authors make a more detailed classification of sampling sites and check the difference between north and south China, and that between rural and urban sites.

Response: Thank for reviewer's suggestion. (Line 459-486) Indeed, the higher temperature in

summer promoted the oxidation of precursors to sulfate and nitrate, while the dense rainfall could scavenge and washout, the particles and then decrease the concentrations of sulfate and nitrate. We agreed with reviewer suggestion. We have classified all of the cities into South and North China and rural and urban sites. Overall, the acidic ions in both of North China and South China exhibited the higher concentrations in winter and spring, and the lower ones in summer. However, the NO_3^- concentration in South China displayed a slight difference, which showed the highest one in spring. It was assumed that the relatively scarce precipitation in spring could be responsible for the higher NO_3^- level.

Comment 7: Line 482. The Ca was extremely high in summer, but the dust emissions might not be high in summer due to precipitation. I guess there are some other reasons besides those mentioned by the authors.

Response: Thank for reviewer's suggestion. (Line 490) Based on the reference review, many previous studies have found that the Ca^{2+} in the precipitation was higher in summer compared with other seasons (Niu et al., 2014). It was widely acknowledged that soil-derived crust particulates in the atmosphere were deposited concurrent with the initial rainfall events occurring in summer. Indeed, the dust emission from desert was fewer in summer, while the road dust cannot be neglected. Lyu et al. (2016) demonstrated that the high temperature coupled with strong wind caused the lower water content in the road, leading to higher tendency of road dust re-suspension in the Wuhan summer.

Comment 8: Lines 664 and 665. Ca emissions could also from some coal burning and industry sources. That means anthropogenic sources could contribute to Ca. I feel that the uncertainty of the method should be discussed here, as you indicate that the contribution from human activities was almost zero for Ca. Moreover, over one third of sulfate was expected to come from natural sources (AF=66.65%), what are they?

Response: I agree with reviewer's suggestion. (Line 722-727) Indeed, there are some uncertainties in the geochemical index method, and thus we have discussed the uncertainty in the last paragraph of section 3.4.1. First of all, the background values of Na^+ in the sea and Ca^{2+} in the soil displayed the higher uncertainty, which varied significantly with the study areas. Unfortunately, the background values of Na^+ and Ca^{2+} over China were absent. Besides, the source classification might be not very accurate because many other sources such as forest fire and volcanic eruption were also

ignored. The sulfate generally possesses some natural sources including the contributions of sea-spray, dust emission, forest fire, and volcanic eruption.

Comment 9: Minor issues: Lines 216-217, do the “rain” and “precipitation” mean the same thing in eqs (8) and (9)? Line 223, what is FA? Line 288, Liu or Lu? Line 297-298, why compared with 2000? Should it be 2010? Line 741 increased or decreased? Lines 842-843, rewrite the sentence. It is not clear.

Response: Thank for reviewer’s suggestion. The “rain” and “precipitation” mean the same thing. To avoid the misunderstanding, we have replaced the rain by precipitation. FA means factor analysis. Line 294-295, the Liu has been revised to Lu. Line 304-305, we compared the pH value with that in 2000 rather than 2010. It was assumed that few references concerned about the pH value over China. To date, we only found a paper about the pH value before 2000, and thus we compare with the pH value with that in 2000, and explore the factors for the pH difference. Line 766, the “increased” has been replaced by “decreased”. Line 867-868: The sentences has been replaced by “The results of SR analysis and GWR method implied that GIP, TEC, vehicle ownership, and N fertilizer use were main factors for SO_4^{2-} , NO_3^- , NH_4^+ , and F^- in the precipitation”.

Reviewer #2:

Comment: I noticed that the authors improved their manuscript substantially after careful revision based on reviewer’s comments. I am satisfied at their revision. The paper now can be accepted for publication in ACP as its current form.

Response: Thank for reviewer’s suggestion. I have uploaded the revised manuscript to the system.

1 **The wet deposition of the inorganic ions in the 320 cities across**
2 **China: spatiotemporal variation, source apportionment, and**
3 **dominant factors**

4 Rui Li^a, Lulu Cui^a, Yilong Zhao^a, Ziyu Zhang^a, Tianming Sun^a, Junlin Li^a, Wenhui

5 Zhou^a, Ya Meng^a, Kan Huang^a, Hongbo Fu^{a,b,c,*}

带格式的: 上标

6 ^a Shanghai Key Laboratory of Atmospheric Particle Pollution and Prevention, Department of
7 Environmental Science & Engineering, Institute of Atmospheric Sciences, Fudan University,
8 Shanghai, 200433, P.R. China

9 ^b Shanghai Institute of Pollution Control and Ecological Security, Shanghai 200092, P.R. China

10 ^c Collaborative Innovation Center of Atmospheric Environment and Equipment Technology
11 (CICAEET), Nanjing University of Information Science and Technology, Nanjing 210044, P.R.
12 China

13 **Corresponding author**

14 fuhb@fudan.edu.cn

15 **Abstract**

16 The acid deposition has been considered to be a severe environmental issue in China. The pH,
17 electrical conductivity (EC), and the concentrations of the water soluble ions (NO₃⁻, Cl⁻, Ca²⁺, K⁺,
18 F⁻, NH₄⁺, Mg²⁺, SO₄²⁻, and Na⁺) in the precipitation samples collected from the 320 cities during
19 2011-2016 across the whole China were measured. The mean concentrations of F⁻, NO₃⁻ and SO₄²⁻
20 were in the order of winter (6.10, 19.44 and 45.74 μeq/L) > spring (3.45, 13.83, and 42.61 μeq/L) >
21 autumn (2.67, 9.73, and 28.85 μeq/L) > summer (2.04, 7.66, and 19.26 μeq/L). The secondary ions
22 (SO₄²⁻, NO₃⁻ and NH₄⁺), and F⁻ peaked in Yangtze River Delta (YRD) and Sichuan basin (SB). The

23 crustal ions (i.e., Ca^{2+} , Mg^{2+}), Na^+ , and Cl^- showed the highest concentrations in the semi-arid
24 regions and the coastal cities, respectively. The statistical methods confirmed that the mean
25 anthropogenic contribution ratios to SO_4^{2-} , F^- , NO_3^- , and NH_4^+ at a national scale were 46.12%,
26 71.02%, 79.10%, and 82.40%, respectively. However, Mg^{2+} (70.51%), K^+ (77.44%), and Ca^{2+}
27 (82.17%) were mostly originated from the crustal source. Both Na^+ (70.54%) and Cl^- (60.42%) were
28 closely linked to the sea-salt aerosols. On the basis of the stepwise regression (SR) analysis, it was
29 proposed that most of the secondary ions and F^- were closely related to gross industrial production
30 (GIP), total energy consumption (TEC), vehicle ownership, and N fertilizer use, but the crustal ions
31 (Ca^{2+} and K^+) were mainly controlled by the dust events. The influence of dust days, air temperature,
32 and wind speed on ions increased from Southeast China (SEC) to Central China, and then to
33 Northwest China (NWC), whereas the influence of socioeconomic factors on acid ions (SO_4^{2-} and
34 NO_3^-) displayed the higher value in East China.

35 **Keywords:** Water-soluble ions; precipitation; spatiotemporal variation; source identification; China

36 1. Introduction

37 Atmospheric wet deposition generally removes efficiently the aerosol particles and dissolved
38 gaseous pollutants from the atmosphere (Garland, 1978; Al-Khashman, 2005; Migliavacca et al.,
39 2005). However, in some regions with severe air pollution, the scavenging of substantial aerosol
40 particles alters the chemical compositions of precipitation and even aggravates the acid deposition
41 (Kuang et al., 2016). Some inorganic ions (i.e., SO_4^{2-} , NO_3^- , NH_4^+ , Ca^{2+}) play significant roles on
42 the terrestrial and aquatic ecosystem via wet deposition; for instance, leading to severe soil (lake)
43 acidification (alkalization), inhibiting the plant growth, and changing the regional climate (Liu et
44 al., 2011; Yan et al., 2010; Larssen and Carmichael, 2000; Larssen et al., 1999). In the past decades,

45 China has been suffered from the severe air pollution along with the population growth and
46 industrialization (Liu et al., 2016a). Therefore, the investigation of the wet deposition status of
47 inorganic ions is of great interest to the public and policy makers (Négrel et al., 2007).

48 A large amount of studies mainly focused on the spatiotemporal variation of the S and N
49 deposition around the world due to their adversely ecological effects in the past decades (Gerson et
50 al., 2016; Clemens 2006; Zhang et al., 2010). Okuda et al. (2005) showed that the SO_4^{2-}
51 concentration in the precipitation exhibited a slight decrease coupling with the decrease of the SO_2
52 concentration in Tokyo during 1990-2012. Hunová et al. (2014) reported that the averagely S
53 deposition flux decreased from 181 kg/ha/year to 100 kg/ha/year in Czech during 1995 and 2011 on
54 the basis of the data in 15 cities. Du et al. (2012) estimated that the wet deposition flux of inorganic
55 nitrogen reached 3.5 kg N/ha/year according to the average of 151 monitoring in the United States
56 during 1985-2012, which were significantly lower than that of China during the same period (11.11-
57 13.87 kg/ha/yr) (Jia et al., 2014).

58 Many researches about the S and N deposition have been extensively performed to date in China
59 in the recent years (Jia et al., 2014; Xu et al., 2015). In the past decades, the anthropogenic emissions
60 of SO_2 , NO_2 , and NH_3 displayed the remarkable increase along with the dramatic increase of fossil
61 fuel and fertilizer consumption in China (Jia et al., 2014; Kuribayashi et al., 2012). It was well
62 documented that the gaseous precursors containing S and N could be transformed into sulfates
63 (SO_4^{2-}), nitrates (NO_3^-), and ammonium (NH_4^+) during ageing in the atmosphere, thereby
64 contributing to the formation of airborne fine particles, of which were considered to be the main
65 reason for the persistent fog and haze pollution in China (Wang et al., 2016a; Qiao et al., 2015). At
66 a city level, Huang et al. (2008) observed that the wet deposition fluxes of SO_4^{2-} , NH_4^+ , and Ca^{2+}

67 displayed the slight decrease from 1986 to 2006 in the urban of Shenzhen, whereas the wet
68 deposition of NO_3^- increased rapidly during the same period. Very recently, Pu et al. (2017) reported
69 that the SO_4^{2-} concentration in the wet deposition of Shangdianzi (a regional background station of
70 Beijing) showed slight decrease during 2003-2014, but the NO_3^- concentration showed an opposite
71 trend. At a regional scale, Pan et al. (2013) observed that the highest S wet deposition was
72 concentrated in the urban and industrial region of Tianjin among of ten sites of North China (NC).
73 Song et al. (2017) suggested that the bulk deposition fluxes were in the order of Chengdu (urban) >
74 Yanting (agricultural area) > Gongga mountain (natural reserve). At a national scale, Jia et al. (2014)
75 firstly found that the wet deposition of N in Southeast China (SEC) showed a significant decrease,
76 whereas it increased slightly in the western of China on the foundation of the data (620 monitoring
77 sites) collected from 120 cities across China during 1990 and 2010. Following this work, Liu et al.
78 (2016) further observed that the serious S deposition (79 monitoring sites) on SEC and Southwest
79 China (SWC). In these studies, the spatial distributions of both S and N were determined using the
80 spatial interpolation method, which generally required substantial monitoring sites (city > 150, and
81 monitoring site > 300). However, these conclusions were obtained based on a small quantity of
82 monitoring sites, which increased the uncertainties of the results. Meanwhile, the monitoring sites
83 in these studies were mainly located on some remote regions such as mountain or rural site rather
84 than the mixture of urban, suburban, and rural sites, which cannot accurately reflect the spatial
85 variations of inorganic ions in China. Moreover, the spatiotemporal variations of other inorganic
86 ions (i.e., K^+ , Ca^+ , Mg^{2+}) remained unclear to date, which were also linked to the acid deposition,
87 as well as the haze pollution in China (Mikhailova et al., 2013; Aloisi et al., 2017; Müller et al.,
88 2015).

89 Based on these field measurements, the ion levels in the deposition across China were believed
90 to be underestimated due to the few ion species measured by previous studies (Liu et al., 2016a),
91 which was closely associated with various emission sources (Kuang et al., 2016). Thus, the source
92 identification should be performed to assess accurately their contributions to the wet deposition
93 (Larssen et al., 1999). Liu et al. (2015b) identified that the Cl^- and NH_4^+ in the precipitation of Tibet
94 were both originated from the marine and crustal source using the geochemical index method. On
95 the basis of the positive matrix factorization (PMF) model, Qiao et al. (2015) showed that fossil fuel
96 combustion and agriculture were the main sources of SO_4^{2-} and NO_3^- in Jiuzhaigou (Sichuan
97 province). In a newly work reported by Leng et al. (2018), they supposed that the combustion of
98 fossil fuels, domestic sewages, and fertilizers were the main sources of the N-bearing ions on the
99 basis of the N isotope analysis. To date, some methods, including geochemical index method,
100 multivariate analyses, and isotope signatures have been utilized to identify the anthropogenic versus
101 natural sources of the inorganic ions in the precipitation. However, these methods suffered from
102 some weaknesses from different standpoints (AlKhatib and Eisenhauer 2017; Shi et al., 2014). For
103 instance, the geochemical index methods cannot estimate the contribution ratios of multiple sources
104 to Ca^{2+} and Na^+ at a spatial scale (Liu et al., 2015b). Despite the advances of multivariate analyses
105 lowering the associated uncertainties, the multi-collinearity still disturbed the predictions of these
106 models (Shi et al., 2014). The isotope signature method was costly and complex, especially for the
107 unconventional stable isotopes (i.e., K, Ca) (AlKhatib and Eisenhauer 2017), which restricted its
108 application at a large scale. Therefore, multiple source apportionment methods should be combined
109 in order to enhance the reliability of the results. Liu et al. (2015) also demonstrated that the
110 geochemical index method coupled with multiple statistics decreased the uncertainties of results.

111 Apart from the source apportionment, the key factor identification for the ions in the wet
112 deposition is also of great importance to reduce the acid deposition. At an early study, Singh and
113 Agrawal (2008) revealed that the significant increase of vehicle emissions contributed to the
114 accumulation of NO₂, which might be an important precursor of acid rain. Allen et al. (2015)
115 observed that some inland cities in arid and semi-arid regions were generally subjected to dust
116 events, which could increase the Ca²⁺ and K⁺ concentrations in the wet deposition. Following this
117 work, Yu et al. (2017a) found that considerable energy consumption, gross domestic production
118 (GDP), and emitted substantial pollutants made China as major regions of acid rain around the world
119 using path analysis and correlation analysis. However, these researches only assessed the limited
120 factors for the inorganic ions in the wet deposition (Yu et al., 2016; Yu et al., 2017a), ignoring the
121 contributions of other socioeconomic and natural factors. Moreover, these researches mainly
122 focused the whole effects of the influential factors on inorganic ions at a national scale, while they
123 did not consider the spatial heterogeneity of the influential factors, resulting possibly in the great
124 deviation of the inorganic ions in the wet deposition for the different regions.

125 Here, the data of nine water-soluble ions in the precipitation including Ca²⁺, Cl⁻, F⁻, K⁺, Mg²⁺,
126 Na⁺, NH₄⁺, NO₃⁻, and SO₄²⁻ in the 320 cities across the whole China were collected during 2011-
127 2016 to examine the characteristics of the main water-soluble ions in the precipitation. Specifically,
128 the objectives of our study were (1) to reveal the spatiotemporal patterns of water-soluble ions in
129 the precipitation recently in China at a national scale; (2) to identify quantitatively the source of the
130 water-soluble ions in the precipitation based on the multiple statistical methods; and (3) to seek out
131 the key factors for the inorganic ions at a spatial scale. This study supplied the systematical data for
132 comprehensive understanding on the inorganic composition in the precipitation based on the long-

133 term field measurement, at a national scale (the 1282 monitoring sites distributed in the 320 cities
134 across the whole China), which was beneficial to the implementation of appropriate strategies to
135 promote environmental protection in China.

136 **2. Materials and methods**

137 2.1 Site description

138 The spatial distribution of field stations in National Acid Deposition Monitoring Network
139 (NADMN) is illustrated in Fig. 1. The selected 1282 monitoring sites are distributed in the 320 cities
140 across 31 provinces. These cities are classified into Northeast China (NEC), NC, SEC, Northwest
141 China (NWC), and Southwest China (SWC) (Tab. S1). Both of NEC and NC show typical
142 temperature monsoon climate, while SEC presents the subtropical monsoon climate. The SWC
143 region suffers from the combined effects of subtropical monsoon climate and tropical monsoon
144 climate. NWC suffers from the temperate continental climate and displays minor rainfall amount.
145 NEC and NC are filled with temperate deciduous forest, whereas SEC is mainly occupied by the
146 subtropical evergreen forest. The subtropical evergreen forest and tropical evergreen forest spread
147 out the SWC region. The NWC is generally filled with expansive grasslands and desert. The
148 latitudes and longitudes of all of 1282 monitoring sites range from 18.25 to 50.78° N, and from 79.57
149 to 129.25° E, respectively. Annual mean rainfall ranges from 10 to 1853 mm and the annual mean
150 air temperature varies between -6.9 and 24.3 °C. The monitoring sites were designed as a mixture
151 of urban and background sites. ~~Most of these sites~~850 monitoring sites are concentrated in urban
152 region, and ~~a few of sites~~432 sites in suburban and rural areas are considered as the background
153 sites.

154 2.2 Sampling and chemical analysis

155 The real-time precipitation was collected by monitors in the field stations as a routine procedure
156 of NADMN. Samples from each monitoring site were collected using wet deposition automatic
157 collectors (diameter 30 cm) installed at 1.5 m above ground level. The cover of the collection
158 instrument opened automatically without delay when the precipitation sensor was activated and
159 closed automatically when precipitation ceased and no water remained on the sensor surface. The
160 sample in each rain event was collected and these samples were collected in all of the monitoring
161 sites simultaneously. Each sample was properly collected during the precipitation event when the
162 wet-only deposition instrument was under the normal condition. After the sampling, the pH and EC
163 values of the samples were measured immediately. The sample pH was measured using a pH meter
164 (MP-6p, HACH, USA) at 20–25°C. The EC value of the precipitation samples was determined by
165 an EC meter (CyberScan, CON1500, USA). After the analysis of pH and EC, all of the samples
166 were contained in the pre-cleaned polyethylene plastic bottles at -18°C in order to prevent the
167 possible transformation by microbes. All of the plastic buckets and the polyethylene plastic bottles
168 were cleaned with deionized water for more than three times and then air-dried in clean room prior
169 to use.

170 All of the precipitation samples were used to analyze the concentrations of the water-soluble
171 ions including NO_3^- , Cl^- , Ca^{2+} , K^+ , F^- , NH_4^+ , Mg^{2+} , SO_4^{2-} , and Na^+ . The microporous membranes
172 (0.45 μm) were employed to remove all of insoluble particulates ($< 0.45\mu\text{m}$) from the precipitation
173 samples before the analysis. The ion concentrations were determined through ion chromatography
174 (Dionex ICS-900) equipped with a conductivity detector (ASRS-ULTRA). The CS12A column and
175 AS11-HC column were applied to determine the cations and anions, respectively. Each sample was
176 measured for more than three times and the relative standard deviation was less than 5% for each

177 ion. Analysis of the blank samples once a month confirmed that the cross contamination in the
178 present research was negligible. For each ion, the analysis of simulated precipitation suggested that
179 the relative bias was lower than 10%.

180 2.3 Data calculation

181 The monthly and annual volume-weighted mean (VWM) concentrations were calculated based
182 on the concentrations of specific ions and precipitation. The monthly and annual VWM
183 concentrations were obtained as follows:

$$184 \quad C_x = \frac{\sum_{i=1}^n (C_i(x) \times P_i)}{\sum_{i=1}^n P_i} \quad (1)$$

185 where C_x denoted the monthly and annual VWM concentration of the given ion; $C_i(x)$ was the
186 concentration of the given ion in the precipitation ($\mu\text{eq/L}$); P_i was the precipitation in individual
187 sample. The monthly and annual VWM pH values were obtained based on the corresponding VWM
188 concentrations of H^+ via Eq. (1).

189 The wet deposition flux of the given ion was calculated using the following Eq. (2)

$$190 \quad D_w = P_t C_w / 100 \quad (2)$$

191 where D_w was the wet deposition flux of the given ion (kg N ha^{-1}); P_t was the total amount of the
192 precipitation events (mm); C_w was the VWM concentration of each ion (mg/L); and 100 was a unit
193 conversion factor.

194 In order to obtain the contributions of various alkaline species to acid neutralization in the
195 precipitation, the neutralization factor (NF) was calculated using the following Eq. (3)-(5)
196 (Kulshrestha et al., 1995):

197
$$NF_{NH_4^+} = \frac{NH_4^+}{NO_3^- + SO_4^{2-}} \quad (3)$$

198
$$NF_{Ca^{2+}} = \frac{Ca^{2+}}{NO_3^- + SO_4^{2-}} \quad (4)$$

199
$$NF_{Mg^{2+}} = \frac{Mg^{2+}}{NO_3^- + SO_4^{2-}} \quad (5)$$

200 2.4 Source apportionment of ionic species in wet deposition

201 The enrichment factor (EF) has been widely applied to estimate the contribution ratios of the
 202 various sources to the major ions in the previous studies (Lawson and Winchester 1979; Cao et al.,
 203 2009; Lu et al., 2011). In the present study, an ion EF in the precipitation relative to the ion in the
 204 sea was calculated using Na as a reference element as follows:

205
$$EF_{sea} = \frac{(X / Na^+)_{precipitation}}{(X / Na^+)_{sea}} \quad (6)$$

206 where EF_{sea} was the enrichment indicator of a given ion in the precipitation relative to the ion in the
 207 sea; X was the ion in the precipitation; $(X/Na^+)_{precipitation}$ represented the ratio of components in the
 208 precipitation; $(X/Na^+)_{sea}$ denoted the ratio of components in the sea (Keene et al., 1986; Turekian,
 209 1968).

210 The EF value of an ion in the precipitation relative to the corresponding ion in the soil was
 211 calculated following Eq. (7):

212
$$EF_{soil} = \frac{(X / Ca^{2+})_{precipitation}}{(X / Ca^{2+})_{soil}} \quad (7)$$

213 where EF_{soil} represented the EF value of an ion in the precipitation relative to the corresponding ion
 214 in the soil; X denoted an ion in the precipitation; $(X/Ca^{2+})_{precipitation}$ was the ratio of components in
 215 the precipitation; $(X/Ca^{2+})_{soil}$ denoted the ratio of components in the soil (Wei et al., 1991; Wei et al.,
 216 1992; Shi et al., 1996; Zhang et al., 2012; Chen et al., 1992).

217 In order to quantify the anthropogenic source versus natural one of ionic species in the
218 precipitation. The fractions of anthropogenic, marine, and crustal source contributed to the ions in
219 the precipitation were calculated as follows:

$$220 \quad SSF = \frac{(X / Na^+)_{sea}}{(X / Na^+)_{precipitation}} \times 100\% \quad (8)$$

$$221 \quad CF = \frac{(X / Ca^{2+})_{soil}}{(X / Ca^{2+})_{precipitation}} \times 100\% \quad (9)$$

$$222 \quad AF = 100\% - SSF - CF \quad (10)$$

223 where *SSF* represented the fraction of sea salt; *CF* denoted the crustal contribution; and *AF* denoted
224 the anthropogenic fraction. *SSF* was recalculated as the difference between 1 and *CF* when *SSF* was
225 greater than 1; *CF* was recalculated as the difference between 1 and *SSF* when *CF* was higher than
226 1.

227 Factor analysis (FA) has been widely employed to determine the contribution ratios of natural
228 and anthropogenic source to ionic species in the precipitation. First of all, FA was applied to reduce
229 the dimension of original variables (measured ion concentrations in samples) and to extract a small
230 number of principal components to analyze the relationships among the observed variables. All of
231 the factors with eigenvalues over 1 were extracted based on the Kaiser-Meyer-Olkin (KMO) test
232 and the Bartlett's test of sphericity, and were rotated using the Varimax method. The FA factor scores
233 and each ion concentration were treated as independent and dependent variables, respectively. The
234 resultant regression coefficients were employed to convert the absolute factor scores and then to
235 calculate the contribution of each PC source (Luo et al., 2015).

236 2.5 The geographical weight regression (GWR) method

237 Although the relationships between the independent variables and the dependent variables could

238 be calculated using correlation analysis and multiple linear regression analysis (MLR), these
239 methods cannot show the spatial variability of regression coefficients. Thus, the GWR method was
240 applied to ~~generate the local regression coefficients for each city, which were then mapped to display~~
241 ~~the spatial variability~~ explore the effects of socioeconomic factors on wet deposition of inorganic
242 ions in consideration of the spatial correlation. —As an indicator to reflect the impacts of
243 socioeconomic factors on inorganic ion depositions. ~~Local-local~~ regression coefficients were
244 obtained using weighted least squares with the following weighting function (Brunsdon et al., 1996):

$$245 \quad \beta(u_i, v_i) = (X^T W(u_i, v_i) X)^{-1} X^T W(u_i, v_i) Y \quad (11)$$

246 where $\beta(u_i, v_i)$ represented the local regression coefficient at city i ; X was the matrix of the
247 influential factors; Y denoted the matrix of the wet deposition fluxes of the water-soluble ions; and
248 $W(u_i, v_i)$ was an n order matrix that the diagonal elements were the spatial weighting of the influential
249 factors. The spatial weight function was calculated via the exponential distance decay form:

$$250 \quad W(u_i, v_i) = \exp(-d^2(u_i, v_i)/b^2) \quad (12)$$

251 where $d(u_i, v_i)$ represented the distance between the location i and j , and b was the kernel bandwidth.

252 2.6 Data source and statistical analysis

253 The data of GDP, gross industrial production (GIP), N fertilizer use, vehicle ownership, urban
254 green space (UGS) during 2011-2016 were collected from China City Statistical Book. Total energy
255 consumption (TEC) during the period were obtained from China Energy Statistical Yearbook, which
256 consisted of the consumption of coal, crude oil, and natural gas. The daily meteorological factors
257 including precipitation, maximum and minimum air temperature, wind speed, air pressure, relative
258 humidity (RH) during 2011-2016 were collected from China Meteorological Data Network. The
259 daily visibility data during 2011-2016 was collected from National Centers for Environmental

260 Prediction (NCEP). The data of dust days were calculated based on the horizon visibility data. The
261 days with the visibility lower than 1 km were treated as the dust days. The daily data of PM_{2.5}, PM₁₀,
262 SO₂, and NO₂ were downloaded from the National Environmental Monitoring Platform
263 (<https://www.aqistudy.cn/historydata/>). These data at a national scale were open access since
264 January 2014. To match the meteorological data at a national scale, the data of air pollutants during
265 2014-2016 were applied to investigate the relationships of the water-soluble ions, meteorological
266 factors, and the air pollutants in the atmosphere (Tab. S2). In addition, the SR analysis was employed
267 to determine the key factors regulating the wet deposition fluxes of the water-soluble ions. All of
268 the statistical analysis were performed by the software package of ArcGIS 10.2, SPSS 21.0, and
269 Origin 8.0 for Windows 10.

270 **3 Results and discussion**

271 3.1 The pH and EC values in the precipitation

272 To obtain the preliminary knowledge about the precipitation characteristics, the basic
273 physiochemical properties including pH and EC of the precipitation samples are presented in Fig.
274 2. The annually pH during 2011 and 2016 ranged from 5.45 ± 0.27 (mean \pm standard deviation) to
275 5.94 ± 0.46 and the mean value was 5.76 (Fig. 2a). Seinfeld (1986) estimated that the precipitation
276 with pH lower than 5.60 was considered as acid rain because the pH value of natural water in
277 equilibrium with atmospheric CO₂ was 5.60. However, the CO₂ level has been increasing in recent
278 years and thus the equilibrium pH has changed (McGlade and Ekins 2015) Therefore, the average
279 CO₂ concentration during 2011-2016 (396.83 ppm) around the world was applied to the present
280 study (<http://www.ipcc.ch/>). The ionization equation of CO₂ include CO₂+H₂O=H₂CO₃ and
281 H₂CO₃=HCO₃⁻+H⁺. The dissociation constant of two equations are 3.47×10^{-2} (K₀) and 4.4×10^{-7} (K₁),

282 respectively. The $(c(\text{H}^+))^2 = K_0 \times K_1 \times P_{\text{CO}_2} = 6.06 \times 10^{-12}$. Therefore, the equilibrium pH was 5.61,
283 which was slightly higher than the current value (pH = 5.60). Herein, 41% of the samples during
284 the measurement showed the pH value below 5.61. Compared with the pH value of the precipitation
285 during 1980-2000 (Wang and Xu 2009), the pH value of the precipitation showed a remarkable
286 increase in recent years. For instance, the pH value in the precipitation of SWC increased from 3.5-
287 4.0 (the mean value of 1980-2000) to 5.87 during 2011-2016. Although some cities in Hunan and
288 Hubei province (e.g., Chengzhou, Erzhou) still suffered from the severe acid deposition, the mean
289 pH values (4.46) of the two provinces during 2011-2016 were slightly higher than those in 1980-
290 2000 (3.5-4.0). It was well known that precipitation pH was associated with the SO₂ and NO_x
291 emissions (Pu et al., 2017). Due to the implementation of SO₂ control measurements since the 11th
292 Five-year Plan, the SO₂ column concentration over China displayed a marked decrease after 2007
293 based on Global Ozone Monitoring Experiment (GOME), reported by Gottwald and Bovensmann
294 (2011). Based on the bottom-up method, Liu et al. (2010) also supposed that SO₂ emission began to
295 decrease since 2007 (Lu et al., 2010), in good agreement with the results obtained from the remote
296 sensing. Besides, nearly all of the power plants built newly and the in-use plants have been required
297 to be equipped with advanced selective catalytic reduction (SCR) or selective non-catalytic
298 reduction (SNCR) since 2010 (Tian et al., 2013; Lu et al., 2011), resulting in a gradual decrease of
299 the NO_x emission after 2010 (China Statistical Yearbook,
300 <http://data.stats.gov.cn/easyquery.htm?cn=C01>). Based on the result of correlation analysis (Tab.
301 S2), the pH value showed the significantly negative correlation with SO₂ and NO₂ in the ambient
302 air especially with the increased RH. Thus, it could be proposed that the pH value of the
303 precipitation in most of the regions of China during 2011 and 2016 were significantly higher than

304 those before 2000 ~~due to because the decreases of~~ the SO₂ and NO_x emissions during 2011-2016
305 were lower than those before 2000.

306 The pH value in the precipitation at a national scale exhibited significantly seasonal variation
307 with the highest value in summer (6.57), followed by autumn (5.64), spring (5.49), and the lowest
308 one in winter (5.32) (Fig. 2b). The seasonal variation of pH values in wet deposition was supposed
309 to be linked with the wash-out effect of precipitation on atmospheric particular matters (Xing et al.,
310 2017), which was supported by the positive relevance between pH and precipitation ($p < 0.01$).
311 Besides, the scavenging atmospheric SO₂ by precipitation may also play an important role in the
312 seasonal variation of the pH values (Wu and Han, 2015). The atmospheric SO₂ concentration was
313 the lowest in summer and the highest in winter. The highest atmospheric SO₂ and sulfate
314 concentrations in winter of the north part of China were partially ascribed to the intensive domestic
315 coal combustion for heating (Liu et al., 2016b; Liu et al., 2017).

316 At a spatial scale across the whole China (Fig. 3a), the pH value of the precipitation presented a
317 gradual increase from SEC to NC and NWC. The relatively low pH values in the precipitation were
318 usually observed in YRD (i.e., Huzhou, Ningbo, and Shanghai), Hunan province (i.e., Changde,
319 Changsha, and Loudi), Hubei province (i.e., Wuhan), and Jiangxi province (i.e., Nanchang, Yichun,
320 and Jingdezhen), but the relatively high pH values occurred in NC and NWC, especially in Xinjiang
321 autonomous region (i.e., Changji, Altai, Urumqi and Aksu). Among of the 320 cities, the lowest one
322 and the highest one were located in Huzhou, (3.20, Zhejiang province), and Altai, (6.82, Xinjiang
323 autonomous region), respectively (Fig. 3). Compared with high acidity in some cities of SEC, the
324 acidity of the precipitation in many cities of NC could be largely neutralized by some alkaline ions
325 because the saline-alkali soils were widely distributed in NC (Wang et al., 2014). Some city

326 atmosphere (i.e., Urumqi and Altay) in Xinjiang autonomous region were frequently attacked by
327 local continental dust particles, diluting the precipitation acidity (Rao et al., 2015).

328 The annually mean EC varied from $10.18 \pm 3.21 \mu\text{S cm}^{-1}$ to $13.33 \pm 3.75 \mu\text{S cm}^{-1}$ during the
329 period (Fig. 2a). The EC value was mainly affected by total water-soluble ions in the precipitation
330 and rainfall amount, of which indirectly reflected the cleanliness of the precipitation and the air
331 pollution status. The decrease of EC in recent years suggested that air pollution in China has been
332 mitigated due to the implementation of special air pollution control measures (Wang et al., 2017;
333 Yang et al., 2016). The EC value also presented distinctly seasonal variation and showed the highest
334 value in spring (Fig. 2c), followed by ones in summer and autumn, and the lowest one in winter,
335 which was apparently different from the seasonal pH variation. Among all of the inorganic ions,
336 only Ca^{2+} displayed notable relationship with EC ($p < 0.01$). It was supposed that many crustal ions
337 such as Ca^{2+} could be lifted up and transported to East China by frequent dust storms in spring and
338 summer, thereby leading to the high EC value in the precipitation (Fu et al., 2014). The mean EC
339 value exhibited a significantly spatial variation with the higher ones in Shizuishan ($36.60 \mu\text{S cm}^{-1}$)
340 and Yinchuan ($24.79 \mu\text{S cm}^{-1}$) (Ningxia autonomous region), Wuwei ($60.01 \mu\text{S cm}^{-1}$) (Gansu
341 province), Edors ($28.72 \mu\text{S cm}^{-1}$) (Inner Mongolia autonomous region), and Aksu ($22.06 \mu\text{S cm}^{-1}$)
342 (Xinjiang autonomous region) and the lower one in some remote regions such as Lhasa ($3.42 \mu\text{S cm}^{-1}$)
343 (Tibet autonomous region), Aba ($2.20 \mu\text{S cm}^{-1}$) (Sichuan province) and Diqing ($2.46 \mu\text{S cm}^{-1}$) (Yunnan
344 province) (Fig. 3b). The lowest and highest EC were observed in Aba ($2.20 \mu\text{S cm}^{-1}$) and Wuwei
345 ($60.01 \mu\text{S cm}^{-1}$), respectively (Fig. 3). The cities in the western and northern of Sichuan province,
346 and the southern of Tibet autonomous region presented the lower EC values due to the sparse
347 population and minimal industrial activity. Although TB has received the effects of the industrial

348 emissions and biomass burning from South Asia via a long-range atmospheric transport, most of the
349 pollutants tended to be deposited on the South of Himalayas except persistent organic pollutants
350 (POPs) (Yang et al., 2016b; Dong et al., 2017). The cities with higher EC was generally close to the
351 Taklamakan and Gobi deserts. Strong winds in these deserts stirred a large amount of dusts, and
352 then caused many dust events, resulting in high loading of Ca^{2+} and Mg^{2+} (Wang et al., 2016d). The
353 positive relationship between wind speed and EC also revealed that strong wind promoted the
354 accumulation of crustal ions over China (Tab. S2).

355 3.2 Chemical composition in the precipitation

356 3.2.1 The inter-annual variation of the water-soluble ions

357 The inter-annual variation of the ionic constituents of the precipitation in China during 2011-2016
358 are summarized in Fig. 4. The concentrations of Na^+ , NO_3^- , and SO_4^{2-} increased from 7.26 ± 2.51 ,
359 11.56 ± 3.71 , and 33.73 ± 7.59 $\mu\text{eq/L}$ to 11.04 ± 4.64 , 13.59 ± 2.63 , and 41.95 ± 8.64 $\mu\text{eq/L}$ during
360 2011 and 2014, respectively (Fig. 4a). However, Na^+ , NO_3^- , and SO_4^{2-} concentrations decreased
361 from the highest ones in 2014 to 9.75 ± 2.89 , 12.29 ± 4.02 , and 30.57 ± 7.43 $\mu\text{eq/L}$ in 2016. The
362 concentrations of Ca^{2+} , NH_4^+ , and Mg^{2+} increased from 31.59 ± 8.29 , 14.84 ± 4.63 , and 8.77 ± 2.42 ,
363 to 58.84 ± 10.31 , 41.33 ± 10.26 , and 10.49 ± 3.07 during 2011-2013 (Fig. 4a), whereas they
364 decreased from the peak values in 2013 to 31.20 ± 8.48 , 18.13 ± 4.84 , and 8.93 ± 2.92 $\mu\text{eq/L}$ in
365 2016, respectively. The F^- concentration exhibited gradual decrease from 3.63 to 2.96 $\mu\text{eq/L}$ during
366 2012-2016. However, the K^+ and Cl^- concentration fluctuated during 2011 and 2016 and did not
367 display regularly annual variation.

368 It was well documented that the SO_4^{2-} concentration was closely associated with the SO_2
369 emissions because SO_2 in the ambient air could be transformed into SO_4^{2-} during aging in the

370 atmosphere (Qiao et al., 2015). In the present study, SO_4^{2-} in the precipitation exhibited a marked
371 correlation with SO_2 in the ambient air ($p < 0.01$), especially with the increased RH (Tab. S2). The
372 total SO_2 emissions in China decreased dramatically due to the installation of the flue gas
373 desulfurization (FGD) systems and the closure of less efficient power plants in China since 2012
374 (Li et al., 2017b). At a national scale, the remarkable decrease of the SO_4^{2-} concentration was
375 observed since 2014, which lagged behind the decrease of the SO_2 emission. Such scenario was
376 widely observed in some developed countries such as Japan (Okuda et al., 2005). However, some
377 cities (i.e., Beijing and Baoding) in NC showed the notable decreases since 2012, which
378 corresponded to the decrease of the total SO_2 emission. It was supposed that the electrostatic
379 precipitators (ESP) and fabric filters (FFs) for the sulfates removal were more widely applied to
380 steel and iron plants, and cement production process, both of which were widely distributed in NC
381 (Hua et al., 2016; Wang et al., 2016b). Moreover, coal has been gradually replaced by natural gas
382 for domestic heating in Beijing, resulting in the less SO_2 emission and thus decreasing the SO_2
383 concentration in the ambient air (Pu et al., 2017). Based on the open data downloaded from National
384 Environmental Monitoring Platform, the annually mean SO_2 concentration in Beijing decreased
385 from $22.0 \mu\text{g}/\text{m}^3$ to $9.29 \mu\text{g}/\text{m}^3$ during 2014-2016, in good agreement with the temporal variation of
386 SO_4^{2-} in the precipitation.

387 The NO_x emission decreased rapidly after the upgrading of oil product quality standards, the
388 import denitrification facilities, and the implementation of low- NO_2 burner technologies (Li et al.,
389 2016; Liu et al., 2017). However, the NO_3^- concentration in the precipitation over China only
390 displayed slight decrease during this period, which was in good agreement with the slight decrease
391 of national NO_2 concentration in the atmosphere (Zhan et al., 2018). It suggested that stricter

带格式的: 下标

带格式的: 下标

392 controls on NO_x emissions from power plants might be counteracted by the increase of power plants
393 and energy consumption (Liu et al. 2015a; Wang et al. 2018). Besides, ~~it~~ it was assumed that the
394 high NO₃⁻ in the precipitation resulted from the increase of motor vehicles (Link et al., 2017). Based
395 on the bottom-up method, the estimated NO_x emissions from vehicle exhausts in China linearly
396 increased by 75% since 1998 (Wu et al., 2016). Shandong suffered from the highest vehicle
397 emissions among all of the provinces, of which the NO_x released from vehicle exhausts in Shandong
398 province increased from 477.6 Gg to 513.8 Gg during 2011-2014 (Sun et al., 2016), corresponding
399 to the annual variation of NO₃⁻ in the precipitation of Jinan and Linyi. The NO₃⁻/SO₄²⁻ value was
400 recognized as an important index to determine the relative importance of nitrate (mobile) vs. sulfate
401 (stationary) emission in the atmosphere (Arimoto et al., 1996). The value of NO₃⁻/SO₄²⁻ at the
402 national scale was still lower than 1, suggesting that the contribution of sulfate to the acidity of the
403 precipitation was still higher than that of NO₃⁻. Nevertheless, the ratio in the precipitation showed a
404 gradual increase from 0.33 to 0.40 during this period, indicating that the precipitation type in China
405 has evolved from sulfuric acid type to a mixed type controlled by sulfuric and nitric acid.

406 The NH₄⁺ level in the precipitation was closely linked to the NH₃ emission because NH₃ tended
407 to be neutralized to form (NH₄)₂SO₄ and NH₄NO₃ in the atmosphere (Zhang et al., 2016). The
408 anthropogenic emission of NH₃ was mainly derived from fertilizer use, livestock manures, vehicle
409 exhausts, and industrial processes (Kang et al., 2016). Wherein, livestock manures and synthetic
410 fertilizer application were considered as two major source of the NH₃ emission, accounting for 80-
411 90% of total emission (Kang et al., 2016; Xu et al., 2016). The nitrogen fertilizer consumption has
412 decreased since 2013 (<http://www.stats.gov.cn/>), which was in good agreement with the variation of
413 the NH₄⁺ concentration in the precipitation. Therefore, the fertilizer consumption could be treated

414 as an important factor for the NH_4^+ level in the precipitation. However, the NH_3 emission from
415 livestock manures estimated by Kang et al. (2016) showed an opposite variation to the NH_4^+ level
416 in the precipitation collected herein. It was probably attributed to the slight decrease of air
417 temperature in the major cities of China during 2011-2013 because the actual NH_3 emission to the
418 atmosphere was sensitive to air temperature (Kang et al., 2016), which has been proved by the
419 correlation analysis (Tab. S2). Apart from the contribution source mentioned above, soil served as
420 major natural sources of the NH_3 emissions (Sun et al., 2014). Teng et al. (2017) demonstrated that
421 urban green space made a great contribution to the NH_3 amount in the atmosphere. In the present
422 study, the urban green space in some cities such as Lianyungang (Jiangsu province) and Qingdao
423 (Shandong province) showed the marked correlation with the NH_4^+ level in the wet deposition.

424 The long-range transport of dust aerosol was considered as the major source of Ca^{2+} and Mg^{2+}
425 in the atmosphere (Fu et al., 2014). Song et al. (2016) reported that the magnitude of dust emissions
426 in spring generally decreased in the past decades. The dust deposition and ambient PM_{10}
427 concentration in the Xinjiang autonomous region also decreased dramatically during 2000-2013
428 (Zhang et al., 2017a). Here, Ca^{2+} and Mg^{2+} in the wet deposition of some cities such as Aksu in
429 Xinjiang autonomous region decreased from 32.37 to 4.80 $\mu\text{eq/L}$ and from 15.80 to 4.81 $\mu\text{eq/L}$
430 during 2011-2016, respectively, corresponding to the decrease of dust deposition. However, the
431 decrease of Ca^{2+} and Mg^{2+} over China significantly lagged behind the reduction of dust deposition.
432 It was well known that the increase of soil particles and dusts due to urbanization might induce the
433 high level of Ca^{2+} and Mg^{2+} in the wet deposition (Lyu et al., 2016). The road mileage in China
434 increased by 25% from 2011 to 2013, while it only showed slight increase (2.52%) during 2013-
435 2016 (<http://www.stats.gov.cn/>). Padoan et al. (2017) also demonstrated that the resuspension of

436 road dust generally showed the highest impact on the emission of the Ca and Mg elements among
437 non-exhaust sources (i.e. tire wear, brake wear, road dust).

438 Both of K^+ and Cl^- were identified as the important tracers for biomass burning and fireworks
439 (Cheng et al., 2014). Nevertheless, the K^+ and Cl^- concentration in the precipitation did not reflect
440 the contribution of biomass burning because biomass burning usually occurred in dry seasons (Zhou
441 et al., 2017b). Furthermore, the K^+ concentration in the precipitation showed significantly
442 relationship with crustal ions (Ca^{2+} ($r = 0.40$, $p < 0.01$) and Mg^{2+} ($r = 0.49$, $p < 0.01$)) (Tab. S2),
443 suggesting that other sources could play important role on the accumulation of K^+ and Cl^- . Chen et
444 al. (2017b) recommended that fugitive dust to be the main source of K^+ when the mitigation
445 measures were seriously implemented. The minor F in the wet deposition served as an indicator of
446 coal combustion because fluorine was generally released from coal combustion (Chen et al., 2013).
447 Recently, the F emission displayed remarkable decrease because more coal-fired power plants were
448 equipped with FGD and dust removal equipment (Zhao and Luo, 2017), which explained the
449 decrease of F in the precipitation of some industrial cities such as Baoding (3.22 to 1.65 during
450 2012-2016), Shijiazhuang (3.18 to 2.73), and Handan (3.88 to 3.53) in Hebei province. Na^+ was
451 generally originated from the transport of sea salt aerosols, fugitive dusts, and the incineration of
452 wastes and fossil fuels (Zhao et al., 2011). The Cl^-/Na^+ value in the precipitation of some coastal
453 cities (i.e. Lishui (1.15), Jiaying (1.20), Dandong (1.18), Wenzhou (1.18)) were similar to the marine
454 equivalent Cl^-/Na^+ ratio (1.17) (Wang et al., 2015a), suggesting that Na^+ in the precipitation of these
455 coastal cities might be derived from ocean. However, the Cl^-/Na^+ ratios in the precipitation of some
456 regions far from the ocean were significantly higher than marine equivalent Cl^-/Na^+ ratio due to the
457 contribution of coal combustion (Liu et al., 2016b; Liu et al., 2017).

458 3.2.2 The seasonal variation of the inorganic ions in the wet deposition

459 ~~Overall, The the~~ mean concentrations of SO_4^{2-} , NO_3^- and F^- in the wet deposition were in the
460 order of winter (SO_4^{2-} , NO_3^- and F^- : 45.74, 19.44 and 6.10 $\mu\text{eq/L}$) > spring (42.61, 13.83, and 3.45
461 $\mu\text{eq/L}$) > autumn (28.85, 9.73, and 2.67 $\mu\text{eq/L}$) > summer (19.26, 7.66, and 2.04 $\mu\text{eq/L}$) (Fig. 4b).

462 ~~However, the seasonal variation of inorganic ions still showed the slight difference between North~~
463 ~~China and South China. The mean concentrations of SO_4^{2-} , NO_3^- and F^- in the precipitation of North~~
464 ~~China displayed the highest in winter (47.88, 13.79, and 5.24 $\mu\text{eq/L}$), followed by those in spring~~
465 ~~(47.02, 10.18, and 3.64 $\mu\text{eq/L}$), autumn (32.20, 10.08, and 2.73 $\mu\text{eq/L}$), and summer (22.75, 6.29,~~
466 ~~and 1.69 $\mu\text{eq/L}$). However, NO_3^- in South China showed the highest level in spring (27.66 $\mu\text{eq/L}$).~~

467 It was well known that SO_4^{2-} and NO_3^- were usually generated via the oxidation of SO_2 and NO_2 in
468 the atmosphere, respectively (Yang et al., 2016). The combustion of fossil fuels for domestic heating
469 in winter probably promoted the accumulations of SO_2 and NO_2 in the atmosphere (Liu et al., 2017;
470 Lu et al., 2010). ~~The cities in North China Some cities in the NC region including Shijiazhuang and~~
471 ~~Zhengzhou~~ showed the higher SO_4^{2-} and NO_3^- levels in the precipitation of winter compared with
472 those in summer, which were in agreement with the seasonal variations of SO_2 and NO_2
473 concentrations in the ambient air. It reflected that the combustion of fossil fuels for domestic heating
474 contributed to the accumulation of SO_4^{2-} and NO_3^- and these ions deposited via the rainfall.

475 ~~Nevertheless, the acidic ions in the cities of South China were not always in agreement with those~~
476 ~~in North because coal combustion for heating in winter was not widespread. The NO_3^- level in South~~
477 ~~China showed the highest one in spring due to the effects of meteorological factors. Moreover, The~~

478 stagnant meteorological conditions including shallow mixing layers, high atmospheric pressure, low
479 precipitation, and low wind speed occurred frequently in winter, thereby trapping more pollutants

带格式的: 下标

带格式的: 上标

带格式的: 下标

带格式的: 上标

480 and elevating the concentrations of SO₂ and NO₂ in the atmosphere (Tai et al., 2010). In contrast,
481 strong solar radiation and turbulent eddies from ocean in summer could promote the dispersion of
482 these pollutants (Antony Chen et al., 2001). For instance, some coastal cities such as Beihai
483 (Guangxi autonomous region) and Haikou (Hainan province) were generally exposed of strong solar
484 radiation and high wind speed, which significantly decreased the SO₄²⁻ and NO₃⁻ concentrations in
485 the precipitation of summer (Beihai: SO₄²⁻ (6.06) and NO₃⁻ (7.37); Haikou: SO₄²⁻ (5.33) and NO₃⁻
486 (4.96)). whereas they usually displayed the higher value in spring due to the scarce rainfall amount.
487 The F⁻ concentration in the precipitation displayed the similarly seasonal variation to SO₄²⁻ and NO₃⁻,
488 which was likely associated with the higher coal consumption for domestic heating in some
489 industrial cities of NC, NWC, and NEC (Ding et al., 2017).

490 The concentrations of Cl⁻, Ca²⁺, K⁺, NH₄⁺, Mg²⁺, and Na⁺ exhibited the highest values in summer,
491 followed by those in spring and autumn, and the lowest one in winter. The higher concentration of
492 NH₄⁺ in the precipitation collected in summer was probably linked to agricultural activities. The
493 widespread utilization of fertilizer in summer have been observed over China (Zhang et al., 2011;
494 Tao et al., 2016), which could increase the NH₃ emission. In addition, the NH₃ emission was
495 sensitive to the air temperature and generally increased with the temperature (Kang et al., 2016).
496 The NH₃ released from agricultural activities could transform to NH₄⁺, especially under the
497 condition of high RH (Li et al., 2013). Thus, the high NH₃ emission and rapid photochemical
498 reaction contribute to the higher NH₄⁺ in the precipitation in summer. However, K⁺, Ca²⁺, and Mg²⁺
499 displayed higher concentrations in spring and summer, which was probably related to the high
500 loading of fugitive dusts (Zhang et al., 2017c). Lyu et al. (2016) demonstrated that the high
501 temperature coupled with strong wind caused the lower water content in the road, leading to higher

502 tendency of dust re-suspension in the Wuhan summer. In the present study, these crustal ions in the
503 precipitation also showed the higher values in the summer of Wuhan. The high concentration of Na⁺
504 and Cl⁻ in spring and summer was probably attributed to the evaporation of sea salt under the
505 condition of high air temperature (Grythe et al., 2014). It was found that Na⁺ in summer were 5.1-
506 10.3 times of those in winter in some coastal cities such as Qingdao (5.96) (Shandong province),
507 Qinhuangdao (9.65) (Hebei province), and Sanya (6.83) (Hainan province).

508 3.2.3 Spatial distribution of the water-soluble ions across the whole China

509 At a spatial scale, the annual mean concentrations of NO₃⁻, Cl⁻, Ca²⁺, K⁺, F⁻, NH₄⁺, Mg²⁺, SO₄²⁻,
510 and Na⁺ ranged from 0.20 to 47.98 µeq/L, from 0.27 to 80.86 µeq/L, from 0.59 to 157.15 µeq/L,
511 from 0.15 to 23.43 µeq/L, from 0.11 to 11.64 µeq/L, from 0.20 to 84.24 µeq/L, from 0.28 to 39.30
512 µeq/L, from 0.29 to 191.95 µeq/L, and from 0.15 to 39.50 µeq/L during 2011-2016, respectively.
513 All of these water-soluble ions displayed significantly spatial variation, as shown in Fig. 5 and Fig.
514 6.

515 The mean concentrations of the secondary ions (NO₃⁻, NH₄⁺, and SO₄²⁻) showed the highest
516 values in YRD (Changzhou (34.53, 73.40, and 80.47 µeq/L) (Fig. 5a-c) and Nanjing (35.62, 17.12,
517 and 49.51 µeq/L) and SB (Chengdu (38.08, 65.19, and 57.16 µeq/L) and Leshan (25.32, 38.99, and
518 61.24 µeq/L)), followed by ones in NC (Jinan (11.67, 16.57, and 58.28 µeq/L) and Anyang (20.46,
519 41.32, and 22.01 µeq/L), and the lowest ones in TB (0.50, 0.91, and 1.44 µeq/L) (Lhasa). Many
520 secondary ions exhibited the high concentrations in YRD because of intensive energy consumption
521 and industrial activities (Zhou et al., 2017a). For instance, the total energy consumption of the
522 Jiangsu province was second to Hebei province among all of the provinces in China (Wang 2014).
523 The SO₂ and NO_x emissions from cement plants and iron and steel industries in Jiangsu and Zhejiang

524 province were significantly higher than those in other provinces (Hua et al., 2016; Wang et al.,
525 2016b), which was in coincident to the spatial agglomeration of the SO₂ and NO₂ concentrations in
526 the ambient air of these provinces It has been reported that the acid deposition pattern have moved
527 from SWC to SEC since 2000s (Yu et al., 2017a). However, SB still possessed high concentrations
528 of secondary ions in the precipitation because of high S content in the local consumed coals (Ren et
529 al., 2006). Besides, the unique topographic conditions and unfavorable diffusion conditions
530 facilitated the deposition of regionally transported pollutants stuck by Qinling mountains and Daba
531 mountain (Kuang et al., 2016), although the energy consumption of Sichuan province was much
532 less than those in other provinces (Tian et al., 2013). Moreover, the steady increase use of fertilizer
533 and livestock manures coupled with high air temperature made SB to be one of the NH₃ emission
534 hotspots (Li et al., 2017a). Nevertheless, some remote areas in NWC and SWC such as Lhasa and
535 Abo showed the lower secondary ions due to sparse population and anthropogenic activities (Li et
536 al., 2007). In these regions, these secondary ions were mainly derived from crustal source, and then
537 deposited concurrently in the rainfall events (Niu et al., 2014). Besides, relatively extensive
538 anthropogenic activities such as increased vehicle exhaust might promote the emissions of
539 secondary ions in the tourist season (Qiao et al., 2017). For instance, the number of tourists in Lhasa
540 have been increasing to 11 million until 2015 ([http://www.xinhuanet.com/fortune/2016-
541 01/13/c_1117763885.htm](http://www.xinhuanet.com/fortune/2016-01/13/c_1117763885.htm)), which could boost the slight increase of secondary ions in the wet
542 deposition.

543 F⁻ showed the higher concentrations in NC, YRD, and SB because many coal-fired power plants
544 and iron and steel industries were mainly concentrated in the Hebei and Jiangsu province (Liu et al.,
545 2015a) (Fig. 6a). Besides, Hebei and Jiangsu were two provinces with much higher coal

546 consumptions (Li et al., 2017), which could release large quantity of F⁻ to the atmosphere. Although
547 the power plants and iron and steel industries were relatively scarce in SB, many large phosphorite
548 mines might increase the F⁻ concentration in the precipitation (Wu et al., 2014). As one of the largest
549 phosphorite mine over China, Jinhe phosphorite mine was close to Chengdu, which significantly
550 increased the F⁻ concentration in the precipitation of Chengdu (9.21 µeq/L). Moreover, the high
551 abundance of F⁻ in the local coal (Mianyang: 269.25 µg/g, Guangan: 1061 µg/g) also contributed to
552 the F⁻ emissions (Dai and Ren, 2006; Wang et al., 2016c; Ren et al., 2006). In addition, the F⁻ in the
553 precipitation showed remarkable relevance with T_{max} based on the correlation analysis ($r = 0.12$, p
554 < 0.05). The annually mean air temperature in SB (17.2 °C) were slightly higher than that in Hebei
555 (14.3 °C) and Jiangsu (16.4 °C) province, thereby boosting the F⁻ emission.

556 The high concentrations of Cl⁻ were mainly concentrated on coastal cities such as Shanghai,
557 Lianyungang (Jiangsu province) and Qingdao (Shandong province) (Fig. 6b), indicating the effect
558 of sea-salt sourced from the ocean (Gu et al., 2011; Allen et al., 2015; Grythe et al., 2014). The high
559 Na⁺ concentration not only focused on these coastal cities (Fig. 6c), but also enrich in some arid and
560 semi-arid cities such as Jinchang (35.08 µeq/L) and Gannan (25.51 µeq/L) (Gansu province). It was
561 assumed that the windblown dust originated from Taklimakan Desert could play a vital role on the
562 enrichment of Na⁺ in Inner Mongolia and Hexi corridor because these regions were located on the
563 downwind direction of dust (Engelbrecht et al., 2016). Meanwhile, the evaporation of salt lakes in
564 West China might promote the Na⁺ enrichment in the precipitation (Bian et al., 2017). Besides, the
565 dust event also promoted the elevation of Ca²⁺, especially in Jiayuguan and Guyuan (Gansu province)
566 (Fig. 6d), both of which were located in the Hexi corridor (Allen et al., 2015). The Mg²⁺ presented
567 higher value in some cities (Handan: 36.63 µeq/L, Liupanshui: 39.30 µeq/L) in the Hebei province

568 and Guizhou province (Fig. 6e). The soil in the Guizhou province possessed the highest Mg
569 concentration (843.33 mg/kg) in China (Li et al., 1992), where the Mg^{2+} stored into the soils could
570 be lifted into the atmosphere by strong wind coupled with severe stony desertification (Jiang et al.,
571 2014). Although the Mg concentration in the soil of Hebei province was slightly lower compared
572 with those of Guizhou province, the bioavailable Mg concentration peaked in Hebei province (Hao
573 et al., 2016), which could be inclined to re-suspend into the atmosphere and then deposit with the
574 rainfall in the warm season.

575 3.2.4 Neutralization capacity of the alkaline ions

576 In order to reveal the most important ion for neutralization (Ca^{2+} , NH_4^+ , and Mg^{2+}) in the
577 precipitation, the relative proportion of three NFs in all of the cities are summarized in Fig. 7. The
578 triangular diagram showed that the contribution of three ions were in the order of Ca^{2+} (51.84%) >
579 NH_4^+ (34.14%) > Mg^{2+} (14.02%). The NF ratios of NH_4^+ and Ca^{2+} in China displayed the highest
580 values in summer, followed by ones in spring and autumn, and the lowest one in winter (Fig. 7a). It
581 was supposed that strong acid neutralization were mainly brought about by the alkaline ions via
582 high rainfall. Besides, the neutralization capacity of the alkaline ions reached higher in spring due
583 to the effects of dust events (Wang et al., 2015b). In the present study, the NFs of NH_4^+ and Ca^{2+} in
584 Beijing (NH_4^+ : 0.57, Ca^{2+} : 0.17) and Baoding (NH_4^+ : 0.56, Ca^{2+} : 0.19) showed the markedly higher
585 values in spring. Zhai and Li (2003) also observed that most frequent dust storms generally occurred
586 in NC in spring. However, the NFs of Mg^{2+} (0.70) showed the highest one in winter. Aside from the
587 temporal difference of neutralization, the NFs presented a significantly spatial variation in China
588 (Fig. 7b). The high NFs of Ca^{2+} were mainly concentrated on some cities in NWC such as
589 Bayingolin (0.57) because these arid and semi-arid regions were exposed of periodic Asian dust

590 intrusions (Yu et al., 2017b). In the case of the typical dust events, the content of crustal species
591 such as Ca increased substantially (Chen et al., 2015). Compared with the other regions, the NFs of
592 NH_4^+ showed the higher value in some cities of SWC such as Chengdu (0.55). Kang et al. (2016)
593 demonstrated that the NH_3 emissions in Sichuan province were significantly higher than those in
594 other provinces of China, accounting for more than 10 % of the total emission from livestock
595 manures. The NFs of Mg^{2+} peaked in NC, which was in good agreement with the higher
596 concentration of Mg^{2+} in the wet deposition of NC. The higher concentration of bioavailable Mg^{2+}
597 in the soil was beneficial to increase the neutralization capacity of Mg^{2+} in the wet deposition (Hao
598 et al., 2016), although the SO_2 and NO_2 emissions in NC were significantly higher than those in
599 other regions (Fu et al., 2016).

600 3.3 Comparisons of pH, EC, and the inorganic ion concentrations with the previous studies

601 The annual mean pH, EC and the inorganic ion levels in the precipitation of some metropolitans
602 across China are summarized in Tab. 1. The mean pH values of the most cities in SEC and SWC
603 (i.e., Shanghai: 4.39 and Wuhan: 4.68) were lower than those in some remote areas such as
604 Jiuzhaigou (5.95) and Yulong mountain (5.94) (Qiao et al., 2018; Niu et al., 2014), while the average
605 pH values of some cities in NC and NWC such as Zhengzhou (6.09) and Urumqi (6.13) were slightly
606 higher than those in remote areas. It was assumed that the remote areas were less affected
607 anthropogenic source except local tourist activities, while high aerosol emissions were mainly
608 centered on some metropolitans of SEC and SWC. The pH of the precipitation in Zhengzhou (pH =
609 6.09) (Henan province) and Urumqi (pH = 6.13) (Xinjiang autonomous region) showed high value
610 compared with some remote regions because of the strong neutralization capacity of alkaline ions
611 (Wang et al., 2014). Besides, the pH values in the wet deposition of most metropolitans in China

612 were also lower than those in some developing countries (e.g., Guaiba: 5.92, Petra: 6.80) (Tab. 1).
613 It was supposed that SO₂ and NO_x emitted from industrial and vehicle emissions in China could be
614 higher than those in some countries such as Brazil and Jordan (Wu and Han 2015). In addition,
615 higher abundance of the neutralizing components in Jordan tended to increase pH of the
616 precipitation. On the other hand, the pH values of the wet deposition in most cities of China were
617 significantly higher than those in some cities of developed countries such as Sardinia (pH = 5.18)
618 (Italy) and Adirondack (pH = 4.50) (United States). It was assumed that many Western countries
619 were faced up with severe acid issue due to the rapid industrialization before 2002 (Sickles II and
620 Shadwick 2015). In addition, the annually mean rainfall amount in some cities of East China were
621 higher than those in Sardinia and Adirondack, which could dilute the acidity of the precipitation
622 (Tsai et al., 2011). The mean EC in the wet deposition of most cities over China were approximate
623 to those in some remote regions (i.e., Yulong Mountain, Jiuzhaigou), and some foreign cities such
624 as Guaiba, Brazil. However, Lanzhou (EC = 58.06 μS cm⁻¹) (Gansu province) and Petra (EC = 160
625 μS cm⁻¹) (Jordan) showed remarkably higher value than other cities, suggesting that the dust
626 cyclones from Taklamakan and Khamaseen played vital roles on the EC and chemical composition
627 in the precipitation (Abed et al., 2009).

628 The concentrations of NO₃⁻, SO₄²⁻, and NH₄⁺ in the most cities of China except Qingdao
629 (Shandong province) and Lhasa (Tibet autonomous region) were significantly higher than those in
630 some natural reserve areas such as Jiuzhaigou, Yulong Mountain, and Nam Co (Qiao et al., 2018;
631 Niu et al., 2014) (Tab. 1), suggesting the local point and non-point emissions in these cities played
632 important roles on the concentrations of inorganic ions in the precipitation. However, the
633 concentrations of these inorganic ions in the most cities were lower than those in foreign cities such

634 as Singapore, Petra (Jordan), Tokyo, and Newark (United States) (Balasubramanian et al., 2001; Al-
635 Khashman et al., 2005; Okuda et al., 2005; Song and Gao 2009), indicating the effects of restricting
636 emissions of air pollutants since Chinese 12th Five-Year Plan (Liu et al., 2016a). However, some
637 cities including Shenyang (Liaoning province) and Chengdu (Sichuan province) were still faced up
638 with severe acid deposition. On the whole, the concentrations of the crustal ions (Ca^{2+} and Mg^{2+})
639 were in the order of the arid and semi-arid cities/regions (Nam Co, Urumqi, Lanzhou, and Petra) >
640 the inland cities and natural reserve regions (Chengdu and Yulong mountain) > the coastal cities
641 (i.e., Guaiba, Singapore, and Tokyo). Kang et al. (2016) reported that Tibetan Plateau have been
642 frequently affected by dust events under the condition of climate change in the past decades, which
643 probably increased the Ca^{2+} and Mg^{2+} levels in Nam Co. However, it should be noted that some
644 coastal cities such as Patras (Greece) and Sardinia (Italy) possessed higher Ca^{2+} and Mg^{2+} levels,
645 which was probably attributed to the long transport of the dust from of the Sahara desert (Kabatas
646 et al. 2014). Cabello et al. (2016) demonstrated that African air masses mostly reached some coastal
647 cities of Mediterranean on the basis of back-trajectory analysis.

648 3.4 The source apportionment of the ions in the precipitation across China

649 3.4.1 EF and geochemical index method

650 The mean values of EFs (seawater and soil), SSF and CF in all of the cities are listed in Tab. 2.
651 The water-soluble ion was treated to be enriched relative to the reference source when the EF value
652 of the ion was significantly higher than 1.00, whereas it was considered to be diluted when the EF
653 value of the ion was not much higher than 1.00. In the present study, the mean EF_{sea} for Na^+ , Cl^- ,
654 SO_4^{2-} , NH_4^+ , K^+ , Mg^{2+} , Ca^{2+} , NO_3^- , and F^- over China were 1.00, 1.13, 7.22, 10.51, 16.16, 18.18,
655 231.56, 3507.49, and 5864.28, suggesting that Cl^- and Na^+ in the precipitation were enriched in the

656 marine origin at a national scale. The mean EF_{soil} of Mg^{2+} , K^+ , Ca^{2+} , Na^+ , SO_4^{2-} , F^- , NO_3^- , NH_4^+ , and
657 Cl^- reached 0.55, 0.83, 1.00, 1.83, 5.13, 9.96, 59.36, 86.31, and 169.88, indicating that Ca^{2+} , K^+ , and
658 Mg^{2+} were considered to be originated from the crustal source. Both of the EF_{sea} for SO_4^{2-} and NO_3^-
659 showed significantly spatial variability and they presented the higher ones in YRD and SB
660 (significantly higher than 1) (Fig. 8a-b), which suggested that both of the ions were not mainly
661 sourced from the sea source. However, EF_{sea} for SO_4^{2-} in some cities such as Nujiang (0.92) and
662 Nanchong (0.81) were lower than 1. It was assumed that the Indian monsoon played an important
663 role on the wet deposition of SO_4^{2-} (Gu et al., 2016). Except SO_4^{2-} and NO_3^- , EF_{sea} for other ions
664 showed relatively uniform distribution at a national scale. EF_{sea} for NH_4^+ , F^- , Ca^{2+} , K^+ , and Mg^{2+} in
665 most of the cities were higher than 1 (Fig. 8c and S1), indicating the effects of anthropogenic source
666 or crustal source. The EF_{sea} for Cl^- presented the lower value in many coastal cities such as Beihai
667 (0.53) and Haikou (0.52), while they were significantly higher than 1 in some inland cities such as
668 Daqing (13.11). The spatial variability of EF_{sea} for Cl^- confirmed the spatial difference of Cl^-/Na^+
669 between coastal cities and inland ones mentioned above. Compared with EF_{sea} , the EF_{soil} of ions
670 generally displayed remarkably spatial variation. The EF_{soil} of SO_4^{2-} , NO_3^- , F^- , and Cl^- showed
671 notably higher values in SEC, implicating the effects of industrial activity (Fig. 8a-b and S2a-b).
672 The EF_{soil} of NH_4^+ presented markedly higher value in the eastern region of Inner Mongolia and
673 Heilongjiang province such as Hegang (325.69) (Fig. 8c) because intensive grazing was beneficial
674 to the NH_3 emission (Kobbing et al., 2014). It was interesting to note that the EF_{soil} of Na^+ showed
675 higher value in some cities around Qinghai Lake and the evaporation of salt lake could contribute
676 to the higher EF_{soil} of Na^+ (Fig. S2c). The EF_{soil} of crustal ions such as Mg^{2+} and K^+ in NWC were
677 close to 1, reflecting the contributions of dust events and soils (Fig. S2e-f).

678 Based on the EF_{sea} and EF_{soil} , the estimated SSF, CF, and AF of ions are depicted in Fig. 9, S3,
679 and S4. The mean SSF values of NO_3^- , F, Ca^{2+} , NH_4^+ , Mg^{2+} , K^+ , SO_4^{2-} , Cl^- , and Na^+ were 0%,
680 0.02%, 0.06%, 0.10%, 2.94%, 4.88%, 13.85%, 88.31%, and 100%, respectively. The average CF
681 values of NH_4^+ , NO_3^- , Cl^- , F, SO_4^{2-} , Na^+ , K^+ , Mg^{2+} , and Ca^{2+} reached 0.01%, 0.02%, 0.59%, 10.04%,
682 19.50%, 35.34%, 95.12%, 97.06%, and 99.94%, respectively. The AF value was considered to be
683 the contribution ratio of each ion except SSF and CF. The AF values of Ca^{2+} , K^+ , Mg^{2+} , Na^+ , Cl^- ,
684 SO_4^{2-} , F, NH_4^+ , and NO_3^- reached 0%, 0%, 0%, 0%, 11.10%, 66.65%, 89.94%, 99.89%, and 99.98%,
685 respectively. The results suggested that NO_3^- , SO_4^{2-} , NH_4^+ , and F were mainly sourced from
686 anthropogenic activities based on minor SSF and CF. It was well documented that the combustion
687 of fossil fuels, iron and steel industrial emission, and vehicle exhaust were main sources of SO_4^{2-}
688 and NO_3^- across China (Song et al., 2006; Yang et al., 2016). In the present study, the AF values of
689 NO_3^- in all of cities were higher than 90%, and those of SO_4^{2-} in half of the cities were higher than
690 60%. Besides, the utility of nitrogen fertilization, and human and livestock excretions were treated
691 as the main source of NH_4^+ emission over China (Cao et al., 2009). Herein, 82.5% of cities across
692 China showed the higher AF value of NH_4^+ (> 90%). Ca^{2+} , K^+ , and Mg^{2+} were mainly derived from
693 crustal origin based on the high CF values. Although the K^+ concentration in the fine particles was
694 usually sourced from biomass burning, the component in the coarse particles generally resulted from
695 the soil erosion and dust re-suspension (Cao et al., 2009). The higher CF values of K^+ in most of
696 cities in China such as Aksu (Xinjiang autonomous region) and Bayin (Gansu province) suggested
697 that the wet deposition has become the main removal mechanism for the K^+ in the coarse particles
698 (Lim et al., 1991). The Na^+ and Cl^- ions were mainly originated from sea source because they were
699 main components of sea-salt and sea-spray aerosol (Prather et al., 2013), which was also supported

700 by the higher SSF value.

701 At a spatial scale, the highest AF values of NO_3^- , SO_4^{2-} , NH_4^+ , and F^- were mainly concentrated
702 on East China and SWC (Fig. 9a-c, S3a-c), which was similar to the spatial variation of population.
703 The emissions of aerosols and their precursors released by human activities were mainly
704 concentrated on East China (Fu and Chen 2016), thereby leading to high AF values of these
705 secondary ions. Indeed, many cities in NC such as Handan and Shijiazhuang showed the higher AF
706 value, which revealed the effects of power plant, non-ferrous smelting, and coal mining. The SSF
707 value of Cl^- exhibited high value in Xinjiang and Qinghai province (i.e., Altay and Haibei), SWC
708 (i.e., Chengdu and Guangan) (Fig. S3d-e), and some coastal cities (i.e., Ningbo and Shanghai). The
709 higher SSF values of Cl^- in SWC and coastal cities of East China were mainly controlled by Indian
710 monsoon and East Asia monsoon driven atmospheric transport, respectively (Gu et al., 2016).
711 However, it was assumed that the higher SSF value of Cl^- in the region close to Qinghai Lake could
712 be linked to the evaporation of saline (Bian et al., 2017). However, the relatively higher CF value
713 of Cl^- was centered on Ningxia autonomous region and Shaanxi province, which was frequently
714 exposed of Aeolian dust especially under the process of wind erosion (Lyu et al., 2017). As the
715 typical crustal ions, K^+ and Mg^{2+} in the most regions of China generally showed high CF values,
716 especially in some cities of SWC (i.e., Guiyang, Zunyi, Zhaotong) (Fig. S4a-d). It was supposed
717 that the severe soil erosion and loss, and rocky desertification frequently observed in Yungui Plateau
718 contributed to the higher CF value in this region (Jiang et al., 2014). The SSF of K^+ and Mg^{2+}
719 showed high values in some coastal cities (i.e., Sanya and Ningbo), and some cities of NWC such
720 as Haibei (Qinghai). The evaporation of salt in East China Sea and Qinghai Lake could play a vital
721 role on the K^+ and Mg^{2+} in these areas (Bian et al., 2017).

722 It should be noted that the geochemical index method showed some uncertainties for the
723 estimation of SSF, CF, and AF. First of all, the background values of Na⁺ in the sea and Ca²⁺ in the
724 soil displayed the higher uncertainty, which varied significantly with the study areas. Unfortunately,
725 the background values of Na⁺ and Ca²⁺ over China were absent. Besides, the source classification
726 might be not very accurate because many other sources such as forest fire, volcanic eruption were
727 ignored.

带格式的: 上标

带格式的: 上标

带格式的: 上标

带格式的: 上标

728 3.4.2 The FA-MLR analysis

729 In order to enhance the reliability of source identification, the FA method was also utilized to
730 identify the source of chemical compositions in the precipitation. The FA results of four seasons are
731 summarized in Tab. 3. Three principal components were extracted from the rainwater samples, all
732 of which explained 85.6% of the total variance. The Kaiser-Meyer-Olkin indicator (0.85) was higher
733 than 0.7, suggesting that three factors extracted in the present study was reasonable. Factor 1
734 grouped NO₃⁻, F⁻, NH₄⁺, and SO₄²⁻, accounting for 52.3% of the variance, which was generally
735 associated with dense anthropogenic activities (Nayebare et al., 2016; Zhang et al., 2017b). Factor
736 2 displayed high loadings of Na⁺ and Cl⁻, indicating the effects of sea-salt and sea-spray aerosol
737 (Gupta et al., 2015). The result was also in good agreement with the high SSF value of Na⁺ and Cl⁻
738 supported by geochemical index method. Factor 3 occupied 9.54% of the total variance and was
739 dominated by Ca²⁺, Mg²⁺, and K⁺. The former two ions were considered to be the important
740 indicators of crustal origin or windblown dust source, which were commonly stored in soils and
741 dusts (Kchih et al., 2015). K⁺ was also observed in urban fugitive dusts, although it was generally
742 considered as an important fingerprint of biomass burning (Shen et al., 2016). As a whole, the result
743 of FA was in coincident with that obtained from the EF and geochemical index method.

744 Although the key origins were isolated via the FA method, the contribution ratio of these
745 sources to the water-soluble ions were still unknown. Thus, the FA-MLR method was further applied
746 to quantify the contribution ratio of several sources to these ions in the 320 cities over China (Fig.
747 10a-d). In four seasons, the mean contributions of the anthropogenic source (NO_3^- , SO_4^{2-} , NH_4^+ , and
748 F^- : 79.10%, 46.12%, 82.40%, and 71.02%) were significantly higher than those of sea source
749 (13.76%, 31.71%, 11.09%, and 11.52%) and crustal origin (7.14%, 22.17%, 6.52%, and 17.46%)
750 for NO_3^- , SO_4^{2-} , NH_4^+ , and F^- . Nevertheless, the contribution ratio was in the order of crustal origin
751 (K^+ , Ca^{2+} , and Mg^{2+} : 77.44%, 82.17%, and 70.51%) > anthropogenic source (13.91%, 10.20%, and
752 18.36%) > sea source (8.65%, 7.64%, and 11.14%) for K^+ , Ca^{2+} , and Mg^{2+} . The sea source was the
753 dominant factor for the accumulation of Na^+ and Cl^- in the rainwater, followed by the crustal origin
754 and the anthropogenic source. In addition, the contribution ratios of three sources showed the slight
755 variation in different seasons (Fig. 10). For instance, the contribution ratio of sea source to most
756 inorganic ions especially Na^+ and Cl^- displayed the highest one in summer, followed by ones in
757 spring and autumn, and the lowest one in winter because the intense evaporation of sea salt in
758 summer was inclined to release more ions to the atmosphere (Teinilä et al., 2014). The contribution
759 ratio of anthropogenic activities presented the notable increase from summer to winter for SO_4^{2-}
760 because of dense coal combustion (20 kg coal/m^2) for domestic heating in winter (Zhao et al., 2016).

761 3.5 The deposition flux of the water-soluble ions and their key factors

762 At a national scale, the annually mean deposition fluxes of NO_3^- , Cl^- , Ca^{2+} , K^+ , F^- , NH_4^+ , Mg^{2+} ,
763 SO_4^{2-} , and Na^+ over China were 13.25, 8.44, 13.80, 2.49, 1.15, 5.90, 2.27, 33.41, and 4.39 kg ha^{-1}
764 yr^{-1} during 2011-2016. The deposition fluxes of NO_3^- , Ca^{2+} , K^+ , NH_4^+ , and Na^+ increased from 13.67
765 to $14.83 \text{ kg ha}^{-1} \text{ yr}^{-1}$, 13.32 to $16.99 \text{ kg ha}^{-1} \text{ yr}^{-1}$, 2.47 to $2.79 \text{ kg ha}^{-1} \text{ yr}^{-1}$, 5.21 to $6.48 \text{ kg ha}^{-1} \text{ yr}^{-1}$,

766 and 4.17 to 5.74 kg ha⁻¹ yr⁻¹ from 2011 to 2013, respectively. However, they ~~increased~~decreased to
767 13.65, 11.01, 2.52, 5.90, and 3.69 kg ha⁻¹ yr⁻¹ in 2016. The wet deposition fluxes of F⁻ and Mg²⁺
768 over China decreased from 1.27 to 0.96 kg ha⁻¹ yr⁻¹ and 2.76 to 1.85 kg ha⁻¹ yr⁻¹ during 2012-2014,
769 respectively. However, they began to increase slightly to 1.17 and 2.15 in 2016, respectively. The
770 wet deposition fluxes of Cl⁻ and SO₄²⁻ showed gradual decrease from 9.80 and 38.87 kg ha⁻¹ yr⁻¹ to
771 8.09 and 26.54 kg ha⁻¹ yr⁻¹ during 2011-2016, respectively. On average, the wet deposition flux of
772 NO₃⁻ were higher by 2.25 times than that of NH₄⁺, which was in contrast to the results of the dry
773 deposition reported by Xu et al. (2015). All of the water-soluble ions showed the highest wet
774 deposition fluxes in summer, followed by ones in spring and autumn, and the lowest ones in winter,
775 which was probably attributed by the high washout effect due to rain in summer (Jia et al., 2014).
776 Based on the results of the correlation analysis, the precipitation showed the significant relationship
777 with the deposition fluxes of the water-soluble ions ($p < 0.05$). In addition, the wet deposition fluxes
778 of the water-soluble ions showed the significantly spatial variation, which were in good agreement
779 with the spatial distribution of the water-soluble ion concentrations except Ca²⁺ (Fig. S5).

780 In order to determine the dominant factors affecting the wet deposition fluxes of the water-
781 soluble ions across China, GDP, GIP, TEC, N fertilizer use, vehicle ownership, UGS, dust days,
782 many meteorological factors (i.e., T_{max}, T_{min}, WS), and air pollutants (i.e., SO₂ and NO₂) were
783 introduced as the explanatory variables. The SR analysis results are depicted in Tab. 4. GIP, vehicle
784 ownership, NO₂, T_{min}, and wind speed served as the key factors affecting apparently the wet
785 deposition of NO₃⁻ at a national scale. The atmospheric emission of NO_x from coal-fired power
786 plants was estimated about 7489.6 kt in 2010, although many newly built power plants were
787 equipped with advanced low NO_x burner (LNB) systems (Tian et al., 2013). Zhang et al. (2014)

788 estimated that NO_x from vehicle emissions reached 4570 kt in 2008, which was considered as the
789 second NO_x source only to industrial activities. The NO_x released from anthropogenic activity could
790 enhance the NO_2 concentration in the ambient air, which could be also transformed to NO_3^- via
791 oxidation in the atmosphere, especially under the condition of high temperature and low WS (Zhang
792 et al., 2016). The wet deposition of NH_4^+ were affected by N fertilizer use, UGS, and NO_2 over
793 China. Russel et al. (1998) recommended early that NH_4^+ in the precipitation was most likely
794 derived from the N fertilizer use via an isotope techniques coupled with back trajectory analysis.
795 Besides, Teng et al. (2017) demonstrated that the emission from UGS was identified to contribute
796 to the atmospheric NH_3 significantly during 60% of the sampling times, which could increase the
797 NH_4^+ concentration in the precipitation due to the photochemical reaction. The wet deposition flux
798 of SO_4^{2-} was closely associated with TEC in the 320 cities of China, respectively. It was supposed
799 that the SO_2 emission were dependent on the use of coal and petroleum (Lu et al., 2010). While
800 terrestrial petroleum emissions have declined in recent years, the emissions from international
801 shipping have offset the decrease of terrestrial petroleum (Smith et al., 2011). In the present study,
802 the deposition of some crustal ions were linked to the dust days because they were mainly derived
803 from the dust storm or soil (Deshmukh et al., 2011; Zhang et al., 2011). The Fdeposition was
804 associated with GIP due to the contributions of the coal-fired power plant fly ash and industrial raw
805 material (Kong et al., 2011).

806 The GWR method was used to calculate the local regression coefficients in order to determine
807 the dominant factor affecting the deposition of the water-soluble ions at the regional scale (Fig. 11
808 and S6). The mean R^2 of GWR method was 0.50 over China, and the p value was lower than 0.05,
809 which suggested that the GWR method could be applicable to the study. The local regression

810 coefficient of dust days for crustal ions including Ca^{2+} , Cl^- , K^+ , and Mg^{2+} increased from SEC to
811 NWC (Fig. S6a-e), suggesting that dust days played a significant role on the crustal ions in NWC
812 due to high intensity of dust deposition and extremely high WS (Zhang et al., 2017a). The influence
813 of GIP on the F^- and NO_3^- increased from West China to East China, and displayed the higher value
814 in some cities of YRD (i.e., Shanghai, Hangzhou) because many coal-fired power plants, cement
815 plants, and municipal solid waste incineration plants were located in YRD (Hua et al., 2016; Tian et
816 al., 2012; Tian et al., 2014) (Fig. S6f and 11a). The influence of N fertilizer use on NH_4^+ was
817 concentrated on some cities of NEC such as Jiamusi (Heilongjiang province) (Fig. 11b-c), Harbin
818 (Heilongjiang province), Changchun (Jilin province) because the largest commodity grain base were
819 located in Heilongjiang and Jilin province, leading to the higher N fertilizer use (Cheng and Zhang,
820 2005). In contrast to the effects of GIP, the TEC influence increased gradually from SEC to NWC,
821 and showed the highest value in Xinjiang autonomous region (i.e., Altay) (Fig. 11d). It has been
822 demonstrated that an inverted U-shaped curve (Environment Kuznets Curve) between per capita
823 GDP and energy consumption was generally observed during the development of economy (Song
824 et al., 2013; Yang et al., 2017). The Environment Kuznets Curve denoted that the energy
825 consumption displayed positive relationship with per capita GDP in the early stage of development.
826 However, the positive relationship tended to transform into the negative relevance with the
827 development of economy because the reliance on the energy-intensive industries would be reduced
828 in the developed stage (Yang et al., 2017). It was assumed that Xinjiang autonomous region kept at
829 the early stage of the inverted-U curve and largely rested on the energy-intensive industries as the
830 less-developed province (Yang et al., 2017). However, some developed provinces in SEC such as
831 Zhejiang and Jiangsu have sped up structural transformation of the economy and reduce the reliance

832 on the heavy industries. The influence of UGS and vehicle ownership peaked in Shandong province
833 (i.e., Qingdao, Jinan) and YRD (i.e., Shanghai, Hangzhou) (Fig. 11e-f). It was supposed that the
834 UGS and vehicle ownership in these cities showed higher values among all of the 320 cities
835 (National Bureau of Statistics of China). Apart from the effects of socioeconomic factors, the
836 meteorological factors also played significant roles on NO_3^- . The influences of air temperature and
837 WS both increased from East China to West China, and showed the highest values in Xinjiang
838 province (Fig. 11g-h). Zhang et al. (2017a) demonstrated that the strong dust events along with high
839 WS contributed to the neutralization of NO_3^- , although the NO_2 concentrations in some cities of
840 Xinjiang province were significantly higher than other regions of China.

841 4. Conclusions

842 This study newly reported spatiotemporal variation of nine water-soluble ions in the
843 precipitation across the whole China during 2011-2016. The mean pH and EC values varied
844 significantly compared with those during 1980-2000 because the implementation of special air
845 pollution control measures have mitigated the air pollution in China. The concentrations of Na^+ ,
846 NO_3^- , and SO_4^{2-} increased from 7.26 ± 2.51 , 11.56 ± 3.71 , and 33.73 ± 7.59 $\mu\text{eq/L}$ to 11.04 ± 4.64 ,
847 13.59 ± 2.63 , and 41.95 ± 8.64 $\mu\text{eq/L}$ during 2011 and 2014, while they decreased from the highest
848 ones in 2014 to 9.75 ± 2.89 , 12.29 ± 4.02 , and 30.57 ± 7.43 $\mu\text{eq/L}$ in 2016, respectively. The
849 concentrations of Ca^{2+} , NH_4^+ , and Mg^{2+} increased by 86.26%, 178.50%, and 19.71% from 2011 to
850 2013, whereas they decreased from 58.84 ± 10.31 , 41.33 ± 10.26 , and 10.49 ± 3.07 in 2013 to 31.20
851 ± 8.48 , 18.13 ± 4.84 , and 8.93 ± 2.92 $\mu\text{eq/L}$ in 2016, respectively. The concentration of F^- decreased
852 linearly by 5.58%/yr during 2012-2016. The mean concentrations of SO_4^{2-} , NO_3^- and F^- showed the
853 highest values in winter, followed by ones in spring and autumn, and the lowest ones in summer. It

854 was supposed that the dense anthropogenic activities such as domestic combustion for heating and
855 adverse meteorological conditions. The crustal ions (Ca^{2+} , Mg^{2+} , and K^+) peaked in spring and
856 summer, suggesting the contributions of fugitive dusts. The Na^+ and Cl^- were markedly affected by
857 evaporation of sea salt. All of the water-soluble ions in the precipitation exhibited notably spatial
858 variability. The secondary ions (SO_4^{2-} , NO_3^- and NH_4^+), and F⁻ peaked in YRD (i.e., Changzhou,
859 Hangzhou, and Nanjing) owing to the intensive energy consumption and industrial activities. The
860 higher S content in the coal and unfavorable diffusion conditions contributed to the higher
861 concentrations of secondary ions in SB (i.e., Chengdu, Leshan, and Dazhou). The crustal ions and
862 sea-salt ions showed the highest concentrations in semi-arid regions (i.e., Guyuan, Jiayuguan) and
863 coastal cities (i.e., Qingdao, Lianyungang), respectively.

864 The EF method, geochemical index method, and FA-MLR method consistently suggested that
865 NO_3^- , F⁻, NH_4^+ , and SO_4^{2-} were dominated by anthropogenic activities. However, the Na^+ and Cl^-
866 were closely associated with sea-salt aerosol. Ca^{2+} , Mg^{2+} , and K^+ were mostly derived from crustal
867 source. The results of SR analysis and GWR method implied that GIP, TEC, vehicle ownership, and
868 N fertilizer use were main factors for SO_4^{2-} , NO_3^- , NH_4^+ , and F⁻ in the precipitation. However, the
869 crustal ions were significantly affected by dust events. The correlation between influential factors
870 and the ions in the wet deposition showed significantly spatial variability. The influence of dust days
871 on the crustal ions increased from SEC to NWC, whereas the influence of socioeconomic factors on
872 secondary ions showed the highest value in East China.

873 The present study validate the model estimations of the water-soluble ions deposition at a
874 national scale, and provide the fundamental data for the prevention and control of acid deposition
875 and air pollution. However, there were several plausible contributors to the uncertainty. First of all,

带格式的: 字体: (默认) Times New Roman

876 the monitoring sites were distributed unevenly and relatively scarce sites were located in Northwest
877 China. Moreover, the limited independent variables were included into the models. Thus, further
878 studies were required to establish more representative monitoring sites and incorporate more
879 variables to reduce the uncertainty associated with the ions deposition.

880 **Acknowledgements**

881 This work was supported by National Key R&D Program of China (2016YFC0202700), National
882 Natural Science Foundation of China (Nos. 91744205, 21777025, 21577022, 21177026),
883 International cooperation project of Shanghai municipal government (15520711200), and Marie
884 Skłodowska-Curie Actions (690958-MARSU-RISE-2015). The meteorological data are available at
885 <http://data.cma.cn/>. The socioeconomic data are collected from <http://www.stats.gov.cn/>.

886

References

- Abed, A.M., Kuisi, M.A., Khair, H.A.: Characterization of the Khamaseen (spring) dust in Jordan, Atmos. Environ. 43, 2868-2876, <https://doi.org/10.1016/j.atmosenv.2009.03.015>, 2009.
- AlKhatib, M. and Eisenhauer, A.: Calcium and strontium isotope fractionation during precipitation from aqueous solutions as a function of temperature and reaction rate; II. Aragonite. 209, 320-342, 2017.
- Al-Khashman, O. A.: Study of chemical composition in wet atmospheric precipitation in Eshidiya area, Jordan, Atmos. Environ. 39(33), 6175-6183, <https://doi.org/10.1016/j.atmosenv.2005.06.056>, 2005.
- Allen, H. M., Draper, D.C., Ayres, B.R., Ault, R., Bondy, A., Takahama, S., Modini, R.L., Baumann, K., Edgerton, E., and Knote, C.: Influence of crustal dust and sea spray supermicron particle concentrations and acidity on inorganic NO_3^- aerosol during the 2013 Southern Oxidant and Aerosol Study, Atmos. Chem. Phys., 15(18), 10669-10685, <https://www.atmos-chem-phys.net/15/10669/2015/>, 2015.
- Aloisi, I., G. Cai, C. Faleri, L. Navazio, D. Serafini-Fracassini, and S. Del Duca.: Spermine regulates pollen tube growth by modulating Ca^{2+} -dependent actin organization and cell wall structure, Front Plant Sci, 8, 1701, 2017.
- Antony Chen, L. W., B. G. Doddridge, R. R. Dickerson, J. C. Chow, P. K. Mueller, J. Quinn, and W. A. Butler.: Seasonal variations in elemental carbon aerosol, carbon monoxide and sulfur dioxide: Implications for sources, Geophys. Res. Lett., 28(9), 1711-1714, <https://doi.org/10.1029/2000GL012354>, 2001.
- Arimoto, R., R. Duce, D. Savoie, J. Prospero, R. Talbot, J. Cullen, U. Tomza, N. Lewis, and B. Ray.: Relationships among aerosol constituents from Asia and the North Pacific during PEM - West A, J. Geophys. Res., 101(D1), 2011-2023, <https://doi.org/10.1029/95JD01071>, 1996.
- Bao, G., Q. Ao, Q. Li, Y. Bao, Y. Zheng, X. Feng, and X. Ding.: Physiological Characteristics of *Medicago sativa* L. in Response to Acid Deposition and Freeze-Thaw Stress, Water Air Soil Poll., 228(9),

376, 2017.

Balasubramanian, R., Victor, T., Chun, N.: Chemical and statistical analysis of precipitation in Singapore. *Water Air Soil Poll.* 130, 451-456, 2001.

Baumbach, G., Vogt, U.: Experimental determination of the effect of mountain-valley breeze circulation on air pollution in the vicinity of Freiburg. *Atmos. Environ.* 33, 4019-4027, [https://doi.org/10.1016/S1352-2310\(99\)00143-0](https://doi.org/10.1016/S1352-2310(99)00143-0), 1999.

Beniston.: Environmental change in mountains and uplands, 2016.

Bian, S., D. Li, D. Gao, J. Peng, Y. Dong, and W. Li.: Hydrometallurgical processing of lithium, potassium, and boron for the comprehensive utilization of Da Qaidam lake brine via natural evaporation and freezing, *Hydrometallurgy*, 173, 80-83, 2017.

Bowden, R. D., E. Davidson, K. Savage, C. Arabia, and P. Steudler.: Chronic nitrogen additions reduce total soil respiration and microbial respiration in temperate forest soils at the Harvard Forest, *Forest Ecol Manag.*, 196(1), 43-56, 2004.

Cao, Y.-Z., S. Wang, G. Zhang, J. Luo, and S. Lu.: Chemical characteristics of wet precipitation at an urban site of Guangzhou, South China, *Atmos. Res.*, 94(3), 462-469, <https://doi.org/10.1016/j.atmosres.2009.07.004>, 2009.

Cabello, M., Orza, J.A.G., Duenas, C., Liger, E., Gordo, E., Canete, S.: Back-trajectory analysis of African dust outbreaks at a coastal city in southern Spain: Selection of starting heights and assessment of African and concurrent Mediterranean contributions, *Atmos. Environ.*, 140, 10-21, <https://doi.org/10.1016/j.atmosenv.2016.05.047>, 2016.

Chen, J., C. Li, Z. Ristovski, A. Milic, Y. Gu, M. S. Islam, S. Wang, J. Hao, H. Zhang, and C. He.: A review of biomass burning: Emissions and impacts on air quality, health and climate in China, *Sci. Total*

Environ., 579, 1000-1034, <https://doi.org/10.1016/j.scitotenv.2016.11.025>, 2017a.

Chen, J., G. Liu, Y. Kang, B. Wu, R. Sun, C. Zhou, and D. Wu.: Atmospheric emissions of F, As, Se, Hg, and Sb from coal-fired power and heat generation in China, *Chemosphere*, 90(6), 1925-1932, <https://doi.org/10.1016/j.chemosphere.2012.10.032>, 2013.

Chen, P., T. Wang, X. Lu, Y. Yu, M. Kasoar, M. Xie, and B. Zhuang.: Source apportionment of size-fractionated particles during the 2013 Asian Youth Games and the 2014 Youth Olympic Games in Nanjing, China, *Sci. Total Environ.*, 579, 860-870, <https://doi.org/10.1016/j.scitotenv.2016.11.014>, 2017b.

Chen, Y., B. Luo, and S.-d. Xie.: Characteristics of the long-range transport dust events in Chengdu, Southwest China, *Atmos. Environ.*, 122, 713-722, <https://doi.org/10.1016/j.atmosenv.2015.10.045>, 2015.

Cheng, Y.-q., and P. Zhang.: Regional patterns changes of Chinese grain production and response of commodity grain base in northeast China, *Scientia Geographica Sinica*, 25(5), 514, 2005.

Cheng, Y., G. Engling, K.-b. He, F.-k. Duan, Z.-y. Du, Y.-l. Ma, L.-l. Liang, Z.-f. Lu, J.-m. Liu, and M. Zheng.: The characteristics of Beijing aerosol during two distinct episodes: Impacts of biomass burning and fireworks, *Environ. Pollut.*, 185, 149-157, <https://doi.org/10.1016/j.envpol.2013.10.037>, 2014.

Chen, Z.J., Chen, C.X., Liu, Y.Q., Lin, Z.S.: The background values and characteristics of soil elements in Fujian province. *Environ. Monit. China*, 8, 107-110, 1992.

Cong, Z., S. Kang, and K. Kawamura (2016), The long-range transport of atmospheric aerosols from South Asia to Himalayas, paper presented at EGU General Assembly Conference Abstracts.

Clemens, S.: Toxic metal accumulation, responses to exposure and mechanisms of tolerance in plants, 88, 1707-1719, 2006.

Dai, S., and D. Ren.: Fluorine concentration of coals in China-an estimation considering coal reserves,

Fuel, 85(7), 929-935, 2006.

Deshmukh, D. K., M. K. Deb, Y. I. Tsai, and S. L. Mkoma.: Water soluble ions in PM_{2.5} and PM₁ aerosols in Durg city, Chhattisgarh, India, Aerosol Air Qual. Res, 11, 696-708, 10.4209/aaqr.2011.03.0023, 2011.

Ding, X., L. Kong, C. Du, A. Zhanzakova, H. Fu, X. Tang, L. Wang, X. Yang, J. Chen, and T. Cheng.: Characteristics of size-resolved atmospheric inorganic and carbonaceous aerosols in urban Shanghai, Atmos. Environ., 167, 625-641, <https://doi.org/10.1016/j.atmosenv.2017.08.043>, 2017.

Dong, Z.W., Kang, S.C., Guo, J.M., Zhang, Q.G., Wang, X.J., Qi, D.H.: Composition and mixing states of brown haze particle over the Himalayas along two transboundary south-north transects, Atmos. Environ., 156, 24-35, <https://doi.org/10.1016/j.atmosenv.2017.02.029>, 2017.

Driscoll, C. T., K. M. Driscoll, M. J. Mitchell, and D. J. Raynal.: Effects of acidic deposition on forest and aquatic ecosystems in New York State, Environ. Pollut., 123(3), 327-336, [https://doi.org/10.1016/S0269-7491\(03\)00019-8](https://doi.org/10.1016/S0269-7491(03)00019-8), 2003.

Du, E.Z., Vries, W.D., Galloway, J.N., Hu, X.Y., Fang, J.Y.: Changes in wet nitrogen deposition in the United States between 1985 and 2012, Environ. Res. Lett., 9, 095004, <https://doi.org/10.1088/1748-9326/9/9/095004>, 2014.

Emmett, B.: The impact of nitrogen on forest soils and feedbacks on tree growth, in Forest Growth Responses to the Pollution Climate of the 21st Century, edited, pp. 65-74, Springer, 1999.

Engelbrecht, P. J., Moosmüller, H., Pincock, S., Jayanty, R.K.M., Lersch, T., Casuccio, G.: Technical note: Mineralogical, chemical, morphological, and optical interrelationships of mineral dust re-suspensions. Atmos. Chem. Phys. 16, 10809–10830, <https://www.atmos-chem-phys.net/16/10809/2016/>, 2016.

Fornaro, A., Gutz, I.G.R.: Wet deposition and related atmospheric chemistry in the São Paulo metropolis,

Brazil: part 2-contribution of formic and acetic acids. *Atmos. Environ.* 37, 117-128, [https://doi.org/10.1016/S1352-2310\(02\)00885-3](https://doi.org/10.1016/S1352-2310(02)00885-3), 2003.

Fu, H., G. Shang, J. Lin, Y. Hu, Q. Hu, L. Guo, Y. Zhang, and J. Chen.: Fractional iron solubility of aerosol particles enhanced by biomass burning and ship emission in Shanghai, East China, *Sci. Total Environ.*, 481, 377-391, <https://doi.org/10.1016/j.scitotenv.2014.01.118>, 2014.

Fu, H.B., Chen, J.M.: Formation, features and controlling strategies of severe haze-fog pollutions in China, *Sci. Total Environ.*, 578, 121-138, <https://doi.org/10.1016/j.scitotenv.2016.10.201>, 2016.

Garland, J.A.: Dry and wet removal of sulphur from the atmosphere, *Sulfur in the Atmosphere*, 349-362, 1978.

Gerson, J. R., C. T. Driscoll, and K. M. Roy.: Patterns of nutrient dynamics in Adirondack lakes recovering from acid deposition, *Ecol. Appl.*, 26(6), 1758-1770, 2016.

Glavas, S., Moschonas, N.: Origin of observed acidic-alkaline rains in a wet-only precipitation study in a Mediterranean coastal site, Patras, Greece. *Atmos. Environ.* 36, 3089-3099, [https://doi.org/10.1016/S1352-2310\(02\)00262-5](https://doi.org/10.1016/S1352-2310(02)00262-5), 2002.

Gottwald, M., Bovensmann, H.: *SCIAMACHY: Exploring the Changing Earth's Atmosphere*, first ed. Springer (ISBN 978-9-481-9895-5), 2011.

Grythe, H., J. Ström, R. Krejci, P. Quinn, and A. Stohl.: A review of sea-spray aerosol source functions using a large global set of sea salt aerosol concentration measurements, *Atmos. Chem. Phys.*, 14(3), 1277, <https://www.atmos-chem-phys.net/14/1277/2014/>, 2014.

Gu, J., Pitz, M., Schnelle-Kreis, J., Diemer, J., Reller, A., Zimmermann, R., Soentgen, J., Stoelzel, M., Wichmann, H.E., Peters, A., Cyrys, J.: Source apportionment of ambient particles: comparison of positive matrix factorization analysis applied to particle size distribution and chemical composition data.

Atmos. Environ. 45, 1849-1857, <https://doi.org/10.1016/j.atmosenv.2011.01.009>, 2011.

Gu, Y., H. Liao, and J. Bian.: Summertime nitrate aerosol in the upper troposphere and lower stratosphere over the Tibetan Plateau and the South Asian summer monsoon region, *Atmos. Chem. Phys.*, 16(11), 6641-6663, <https://doi.org/10.5194/acp-16-6641-2016>, 2016.

Gupta, D., H.-J. Eom, H.-R. Cho, and C.-U. Ro.: Hygroscopic behavior of NaCl-MgCl₂ mixture particles as nascent sea-spray aerosol surrogates and observation of efflorescence during humidification, *Atmos. Chem. Phys.*, 15(19), 11273-11290, <https://doi.org/10.5194/acp-15-11273-2015>, 2015.

Hao, G.J., Zhou, J.Q., Fang, H.L.: Applicability of AB-DTPA method for determining the available content of multi-element in typical soils in China, *Acta Agr. Shanghai (in Chinese)*, 32, 100-107, 2016.

Hua, S., H. Tian, K. Wang, C. Zhu, J. Gao, Y. Ma, Y. Xue, Y. Wang, S. Duan, and J. Zhou.: Atmospheric emission inventory of hazardous air pollutants from China's cement plants: Temporal trends, spatial variation characteristics and scenario projections, *Atmos. Environ.*, 128, 1-9, <https://doi.org/10.1016/j.atmosenv.2015.12.056>, 2016.

Hunová, I., Maznová, J., Kurfürst, P.: Trends in atmospheric deposition fluxes of sulphur and nitrogen in Czech forests, *Environ. Pollut.*, 184, 668-675, <https://doi.org/10.1016/j.envpol.2013.05.013>, 2014.

Ito, M., Mitchell, M., Driscoll, C.T.: Spatial patterns of precipitation quantity and chemistry and air temperature in the Adirondack region of New York. *Atmos. Environ.* 36, 1051-1062, [https://doi.org/10.1016/S1352-2310\(01\)00484-8](https://doi.org/10.1016/S1352-2310(01)00484-8), 2002.

Jia, Y., G. Yu, N. He, X. Zhan, H. Fang, W. Sheng, Y. Zuo, D. Zhang, and Q. Wang.: Spatial and decadal variations in inorganic nitrogen wet deposition in China induced by human activity, *Scientific Reports*, 4, <https://doi.org/10.1038/srep03763>, 2014.

Jiang, Z., Y. Lian, and X. Qin.: Rocky desertification in Southwest China: impacts, causes, and

restoration, *Earth-Science Reviews*, 132, 1-12, <https://doi.org/10.1016/j.earscirev.2014.01.005>, 2014.

Kang, Y., M. Liu, Y. Song, X. Huang, H. Yao, X. Cai, H. Zhang, L. Kang, X. Liu, and X. Yan.: High-resolution ammonia emissions inventories in China from 1980 to 2012, *Atmos. Chem. Phys.*, 16(4), 2043-2058, <https://doi.org/10.5194/acp-16-2043-2016>, 2016.

Kang, L.T., Huang, J.P., Chen, S.Y., Wang, X.: Long-term trends of dust events over Tibetan Plateau during 1961–2010, *Atmos. Environ.*, 125, 188-198, <https://doi.org/10.1016/j.atmosenv.2015.10.085>, 2016.

Kabatas, B., Unal, A., Pierce, R.B., Kindap, T., Pozzoli, L.: The contribution of Saharan dust in PM₁₀ concentration levels in Anatolian Peninsula of Turkey, *Sci. Total Environ.*, 488-489, 413-421, <https://doi.org/10.1016/j.scitotenv.2013.12.045>, 2014.

Kchih, H., C. Perrino, and S. Cherif.: Investigation of desert dust contribution to source apportionment of PM₁₀ and PM_{2.5} from a southern Mediterranean coast, *Aerosol Air Qual. Res.* 15(2), 454-464, 10.4209/aaqr.2014.10.0255, 2015.

Keene, W. C., Pszenny, A. A. P., Galloway, J. N., and Hawley, M. E.: Sea-salt corrections and interpretation of constituent ratios in marine precipitation, *J. Geophys. Res.-Atmos.*, 91, 6647–6658, <https://doi.org/10.1029/JD091iD06p06647>, 1986.

Kong, S., Y. Ji, B. Lu, L. Chen, B. Han, Z. Li, and Z. Bai.: Characterization of PM₁₀ source profiles for fugitive dust in Fushun-a city famous for coal, *Atmos. Environ.*, 45(30), 5351-5365, <https://doi.org/10.1016/j.atmosenv.2011.06.050>, 2011.

Kobbing, J.F., Patuzzi, F., Baratieri, M., Beckmann, V., Thevs, N., Zerbe, S.: Economic evaluation of common reed potential for energy production: a case study in Wuliangshai Lake (Inner Mongolia, China). *Biomass Bioenerg.* 70, 315-329, 2014.

Kulshrestha, U.C., Sarkar, A.K., Srivastava, S.S., Parashar, D.C.: Wet-only and bulk deposition studies at New Delhi (India). *Water Air Soil Pollut.*, 85, 2137–2142, 1995.

Kuribayashi, M., T. Ohara, Y. Morino, I. Uno, J.-i. Kurokawa, and H. Hara.: Long-term trends of sulfur deposition in East Asia during 1981-2005, *Atmos. Environ.*, 59, 461-475, <https://doi.org/10.1016/j.atmosenv.2012.04.060>, 2012.

Kuang, F.H., Liu, X.J., Zhu, B., Shen, J., Pan, Y., Su, M.: Wet and dry nitrogen deposition in the central Sichuan Basin of China, *Atmos. Environ.* 143, 39-50, <https://doi.org/10.1016/j.atmosenv.2016.08.032>, 2016.

Lawson, D.R., Winchester, J.W.: A standard crustal aerosol as a reference for elemental enrichment factors, *Atmos. Environ.* 13, 925-930, 1979.

Larssen, T., and G. Carmichael.: Acid rain and acidification in China: the importance of base cation deposition, *Environ. Pollut.*, 110(1), 89-102, [https://doi.org/10.1016/S0269-7491\(99\)00279-1](https://doi.org/10.1016/S0269-7491(99)00279-1), 2000.

Larssen, T., H. M. Seip, A. Semb, J. Mulder, I. P. Muniz, R. D. Vogt, E. Lydersen, V. Angell, T. Dagang, and O. Eilertsen.: Acid deposition and its effects in China: an overview, *Environ. Sci. Poli.*, 2(1), 9-24, 1999.

Leng, Q.M., Cui, J., Zhou, F.W., Du, K., Zhang, L.Y., Fu, C., Liu, Y., Wang, H.B., Shi, G.M., Gao, M., Yang, F.M., He, D.Y.: Wet-only deposition of atmospheric inorganic nitrogen and associated isotopic characteristics in a typical mountain area, southwestern China, *Sci. Environ. Total*, 616, 55-63, <https://doi.org/10.1016/j.scitotenv.2017.10.240>, 2018.

Le Bolloch, O., Guerzoni, S.: Acid and alkaline deposition in precipitation on the western coast of Sardinia, Central Mediterranean (40 N, 81 E). *Water Air Soil Poll.* 85, 2155-2160, 1995.

Li, C.L., Kang, S.C., Zhang, Q.G., Kaspari, S.: Major ionic composition of precipitation in the Nam Co

region, Central Tibetan Plateau. Atmos. Res. 85, 351–360, <https://doi.org/10.1016/j.atmosres.2007.02.006>, 2007.

Li, L., Q. Tan, Y. Zhang, M. Feng, Y. Qu, J. An, and X. Liu.: Characteristics and source apportionment of PM_{2.5} during persistent extreme haze events in Chengdu, southwest China, Environ. Pollut., 230, 718–729, <https://doi.org/10.1016/j.envpol.2017.07.029>, 2017a.

Li, R., L. Cui, J. Li, A. Zhao, H. Fu, Y. Wu, L. Zhang, L. Kong, and J. Chen.: Spatial and temporal variation of particulate matter and gaseous pollutants in China during 2014–2016, Atmos. Environ., 161, 235–246, <https://doi.org/10.1016/j.atmosenv.2017.05.008>, 2017b.

Li, X., L. Wang, D. Ji, T. Wen, Y. Pan, Y. Sun, and Y. Wang.: Characterization of the size-segregated water-soluble inorganic ions in the Jing-Jin-Ji urban agglomeration: Spatial/temporal variability, size distribution and sources, Atmos. Environ., 77, 250–259, <https://doi.org/10.1016/j.atmosenv.2013.03.042>, 2013.

Li, Y., J. Meng, J. Liu, Y. Xu, D. Guan, W. Tao, Y. Huang, and S. Tao.: Interprovincial reliance for improving air quality in China: a case study on black carbon aerosol, Environ. Sci. Technol., 50(7), 4118–4126, 10.1021/acs.est.5b05989, 10.1021/acs.est.5b05989, 2016.

Li, R., Li, J.L., Cui, L.L., Wu, Y., Fu, H.B., Chen, J.M., Chen, M.D.: Atmospheric emissions of Cu and Zn from coal combustion in China: Spatio-temporal distribution, human health effects, and short-term prediction, Environ. Pollut., 229, 724–734, <https://doi.org/10.1016/j.envpol.2017.05.068>, 2017.

Li, Z.Y., Wang, Z.L., Li, R.J., Xu, Q.H.: The analysis of element content in the soil of 29 provinces/municipality/autonomous region in China, Shanghai agriculture technology (in Chinese), 1992.

Li, Z., Ma, Z., vander Kuijp, T., Yuan, Z.W., Huang, L.: A review of soil heavy metal pollution from mines in China: Pollution and health risk assessment, Sci. Total Environ. 468–469, 843–853,

<https://doi.org/10.1016/j.scitotenv.2018.06.068>, 2014.

Lim, B., T. Jickells, and T. Davies.: Sequential sampling of particles, major ions and total trace metals in wet deposition, *Atmospheric Environment. Part A. General Topics*, 25(3-4), 745-762, 1991.

Link, M. F., J. Kim, G. Park, T. Lee, T. Park, Z. B. Babar, K. Sung, P. Kim, S. Kang, and J. S. Kim.: Elevated production of $\text{NH}_4\text{-NO}_3$ from the photochemical processing of vehicle exhaust: Implications for air quality in the Seoul Metropolitan Region, *Atmos. Environ.*, 156, 95-101, <https://doi.org/10.1016/j.atmosenv.2017.02.031>, 2017.

Liu, F., S. Beirle, Q. Zhang, B. Zheng, D. Tong, and K. He.: NO_x emission trends over Chinese cities estimated from OMI observations during 2005 to 2015, *Atmos. Chem. Phys.*, 17(15), 9261-9275, <https://doi.org/10.5194/acp-17-9261-2017>, 2017.

Liu, F., Q. Zhang, D. Tong, B. Zheng, M. Li, H. Huo, and K. He.: High-resolution inventory of technologies, activities, and emissions of coal-fired power plants in China from 1990 to 2010, *Atmos. Chem. Phys.*, 15(23), 13299-13317, <https://doi.org/10.5194/acp-15-13299-2015>, 2015a.

Liu, Y. W., Ri, X., Wang, Y. S., Pan, Y. P., Piao, S. L.: Wet deposition of atmospheric inorganic nitrogen at five remote sites in the Tibetan Plateau, *Atmos. Chem. Phys.*, 15, 11683-11700, <https://doi.org/10.5194/acp-15-11683-2015>, 2015b.

Liu, L., Zhang, X.Y., Wang, S.Q., Zhang, W.T., Lu, X.H.: Bulk sulfur deposition in China, *Atmos. Environ.*, 135, 41-49, <https://doi.org/10.1016/j.atmosenv.2016.04.003>, 2016a.

Liu, P.F., Zhang, C., Mu, Y., Liu, C.T., Xue, C.Y., Ye, C., Liu, J.F., Zhang, Y.Y., Zhang, H.X.: The possible contribution of the periodic emissions from farmers' activities in the North China Plain to atmospheric water-soluble ions in Beijing, *Atmos. Chem. Phys.*, 16, 10097-10109, <https://doi.org/10.5194/acp-16-10097-2016>, 2016b.

Liu, P.F., Zhang, C.L., Xue, C.Y., Mu, Y.J., Liu, J.F., Zhang, Y.Y., Tian, D., Ye, C., Zhang, H.X., Guan, J.: The contribution of residential coal combustion to atmospheric PM_{2.5} in northern China during winter, *Atmos. Chem. Phys.*, 17, 11503–11520, <https://doi.org/10.5194/acp-17-11503-2017>, 2017.

Liu, X., L. Duan, J. Mo, E. Du, J. Shen, X. Lu, Y. Zhang, X. Zhou, C. He, and F. Zhang.: Nitrogen deposition and its ecological impact in China: an overview, *Environ. Pollut.*, 159(10), 2251-2264, <https://doi.org/10.1016/j.envpol.2010.08.002>, 2011.

Liu, X., X. Ju, Y. Zhang, C. He, J. Kopsch, and Z. Fusuo.: Nitrogen deposition in agroecosystems in the Beijing area, *Agr. Ecosyst. Environ.*, 113(1), 370-377, 2006.

Liu, X., Y. Zhang, W. Han, A. Tang, J. Shen, Z. Cui, P. Vitousek, J. W. Erisman, K. Goulding, and P. Christie.: Enhanced nitrogen deposition over China, *Nature*, 494(7438), 459, <https://doi.org/10.1038/nature11917>, 2013.

Lu, X., L. Y. Li, N. Li, G. Yang, D. Luo, and J. Chen.: Chemical characteristics of spring precipitation of Xi'an city, NW China, *Atmos. Environ.*, 45(28), 5058-5063, <https://doi.org/10.1016/j.atmosenv.2011.06.026>, 2011.

Lu, X., Q. Mao, F. S. Gilliam, Y. Luo, and J. Mo.: Nitrogen deposition contributes to soil acidification in tropical ecosystems, *Global Change Biol.*, 20(12), 3790-3801, <https://doi.org/10.1111/gcb.12665>, 2014.

Lu, Z., D. G. Streets, Q. Zhang, S. Wang, G. R. Carmichael, Y. F. Cheng, C. Wei, M. Chin, T. Diehl, and Q. Tan.: Sulfur dioxide emissions in China and sulfur trends in East Asia since 2000, *Atmos. Chem. Phys.*, 10(13), 6311-6331, <https://doi.org/10.5194/acp-10-6311-2010>, 2010.

Luo, X.S., Xue, Y., Wang, Y.L., Cang, L., Xu, B., Ding, J.: Source identification and apportionment of heavy metals in urban soil profiles, *Chemosphere.*, 127, 152-157, <https://doi.org/10.1016/j.chemosphere.2015.01.048>, 2015.

Lyu, X., N. Chen, H. Guo, L. Zeng, W. Zhang, F. Shen, J. Quan, and N. Wang.: Chemical characteristics and causes of airborne particulate pollution in warm seasons in Wuhan, central China, *Atmos. Chem. Phys.*, 16(16), 10671-10687, <https://doi.org/10.5194/acp-16-10671-2016>, 2016.

Lyu, Y., Z. Qu, L. Liu, L. Guo, Y. Yang, X. Hu, Y. Xiong, G. Zhang, M. Zhao, and B. Liang.: Characterization of dustfall in rural and urban sites during three dust storms in northern China, 2010, *Aeolian Res.*, 28, 29-37, 2017.

McGlade, C., Ekins, P.: The geographical distribution of fossil fuels unused when limiting global warming to 2 °C, *Nature*, 517, 187-190, <https://doi.org/10.1038/nature14016>, 2015.

Müller, W. E., E. Tolba, Q. Feng, H. C. Schröder, J. S. Markl, M. Kokkinopoulou, and X. Wang.: Amorphous Ca²⁺ polyphosphate nanoparticles regulate the ATP level in bone-like SaOS-2 cells, *J. Cell Sci.*, 128(11), 2202-2207, 2015.

Migliavacca, D., E. Teixeira, F. Wiegand, A. Machado, and J. Sanchez.: Atmospheric precipitation and chemical composition of an urban site, Guaíba hydrographic basin, Brazil, *Atmos. Environ.*, 39(10), 1829-1844, <https://doi.org/10.1016/j.atmosenv.2004.12.005>, 2005.

Mikhailova, E., M. Goddard, C. Post, M. Schlautman, and J. Galbraith.: Potential contribution of combined atmospheric Ca²⁺ and Mg²⁺ wet deposition within the continental US to soil inorganic carbon sequestration, *Pedosphere*, 23(6), 808-814, 2013.

National Bureau of Statistics of China, 2010-2016 (Chinese).

Négrel, P., C. Guerrot, and R. Millot.: Chemical and strontium isotope characterization of precipitation in France: influence of sources and hydrogeochemical implications, *Isot. Environ. Healt.*, 43(3), 179-196, 2007.

Nayebare, S. R., O. S. Aburizaiza, H. A. Khwaja, A. Siddique, M. M. Hussain, J. Zeb, F. Khatib, D. O.

Carpenter, and D. R. Blake.: Chemical Characterization and Source Apportionment of PM_{2.5} in Rabigh, Saudi Arabia, *Aerosol Air Qual Re.*, 16(12), 3114-3129, 10.4209/aaqr.2015.11.0658, 2016.

Niu, H.W., He, Y.Q., Lu, X.X., Shen, J., Du, J.K., Zhang, T., Pu, T., Xin, H.J., Chang, L.: Chemical composition of precipitation in the Yulong Snow Mountain region, Southwestern China. *Atmos. Res.* 144, 195-206, <https://doi.org/10.1016/j.atmosres.2014.03.010>, 2014.

Okuda, T., T. Iwase, H. Ueda, Y. Suda, S. Tanaka, Y. Dokiya, K. Fushimi, and M. Hosoe.: Long-term trend of chemical constituents in precipitation in Tokyo metropolitan area, Japan, from 1990 to 2002, *Sci. Total Environ.* 339(1), 127-141, <https://doi.org/10.1016/j.scitotenv.2004.07.024>, 2005.

Wang, W.X., Xu, P.J.: Research Progress in Precipitation Chemistry in China, *Progress in Chemistry*, Z1, 2009.

Padoan, E., Ajmone-Marsan, F., Querol, X., Amato, F.: An empirical model to predict road dust emissions based on pavement and traffic characteristics, *Environ. Pollut.* 237, 713-720, <https://doi.org/10.1016/j.envpol.2017.10.115>, 2017.

Pan, Y. P., Wang, Y. S., Tang, G. Q., Du, W.: Spatial distribution and temporal variations of atmospheric sulfur deposition in Northern China: insights into the potential acidification risks, *Atmos. Chem. Phys.* 1675-1688, <https://doi.org/10.5194/acp-13-1675-2013>, 2013.

Prather, K. A., T. H. Bertram, V. H. Grassian, G. B. Deane, M. D. Stokes, P. J. DeMott, L. I. Aluwihare, B. P. Palenik, F. Azam, and J. H. Seinfeld.: Bringing the ocean into the laboratory to probe the chemical complexity of sea spray aerosol, *P. Natl. Acad. Sci. USA.* 110(19), 7550-7555, <https://doi.org/10.1073/pnas.1300262110>, 2013.

Pu, W., W. Quan, Z. Ma, X. Shi, X. Zhao, L. Zhang, Z. Wang, and W. Wang.: Long-term trend of chemical composition of atmospheric precipitation at a regional background station in Northern China, *Sci. Total*

Environ., 580, 1340-1350, <https://doi.org/10.1016/j.scitotenv.2016.12.097>, 2017.

Qiao, T., M. Zhao, G. Xiu, and J. Yu.: Seasonal variations of water soluble composition (WSOC, Hulis and WSIs) in PM₁ and its implications on haze pollution in urban Shanghai, China, Atmos. Environ., 123, 306-314, <https://doi.org/10.1016/j.atmosenv.2015.03.010>, 2015.

Qiao, X., Du, J., Kota, S.H., Ying, Q., Xiao, W.Y., Tang, Y.: Wet deposition of sulfur and nitrogen in Jiuzhaigou National Nature Reserve, Sichuan, China during 2015-2016: Possible effects from regional emission reduction and local tourist activities. 233, 267-277. Environ. Pollut. 233, 267-277, <https://doi.org/10.1016/j.envpol.2017.08.041>, 2018.

Rao, W., G. Han, H. Tan, and S. Jiang.: Chemical and Sr isotopic compositions of precipitation on the Ordos Desert Plateau, Northwest China, Environ. Earth Sci., 74(7), 5759-5771, 2015.

Ren, D., F. Zhao, S. Dai, J. Zhang, and K. Luo.: Trace Element Geochemical in Coal, edited, Science Press, Beijing, China, 2006.

Russell, K. M., J. N. Galloway, S. A. Macko, J. L. Moody, and J. R. Scudlark.: Sources of nitrogen in wet deposition to the Chesapeake Bay region, Atmos. Environ., 32(14), 2453-2465, [https://doi.org/10.1016/S1352-2310\(98\)00044-2](https://doi.org/10.1016/S1352-2310(98)00044-2), 1998.

Seinfeld, J. H.: Atmospheric Chemistry and Physics of Air Pollution John Wiley & Sons, Inc., New York, 50-51, 1986.

Shen, Z., J. Sun, J. Cao, L. Zhang, Q. Zhang, Y. Lei, J. Gao, R.-J. Huang, S. Liu, and Y. Huang.: Chemical profiles of urban fugitive dust PM_{2.5} samples in Northern Chinese cities, Sci. Total Environ., 569, 619-626, <https://doi.org/10.1016/j.scitotenv.2016.06.156>, 2016.

Shi, C.W., Zhao, L.Z., Guo, X.B., Gao, S., Yang, J.P., Li, J.H.: The distribution characteristic and influential factors of background values for elements in Shanxi province, Agro-environmental Protection,

15, 24-28, 1996.

Shi, G.L., Liu, G.R., Peng, X., Wang, Y.N., Tian, Y.Z., Wang, W., Feng, Y.C.: A comparison of multiple combined models for source apportionment, including the PCA/MLR-CMB, UNMIX-CMB and PMF-CMB Models, *Aerosol Air Qual. R.*, 14, 2040-2050, 2014.

Sickles II, J.E., Shadwick, D.S.: Air quality and atmospheric deposition in the eastern US: 20 years of change, *Atmos. Chem. Phys.*, 15, 173-197, <https://doi.org/10.5194/acp-15-173-2015>, 2015.

Simkin, S. M., E. B. Allen, W. D. Bowman, C. M. Clark, J. Belnap, M. L. Brooks, B. S. Cade, S. L. Collins, L. H. Geiser, and F. S. Gilliam.: Conditional vulnerability of plant diversity to atmospheric nitrogen deposition across the United States, *P. Natl. Acad. Sci. USA.*, 113(15), 4086-4091, <https://doi.org/10.1073/pnas.1515241113>, 2016.

Singh, A., Agrawal, M.: Acid rain and its ecological consequences. *J. Environ. Biol.* 29, 15-24, 2008.

Smith, S. J., J. v. Aardenne, Z. Klimont, R. J. Andres, A. Volke, and S. Delgado Arias.: Anthropogenic sulfur dioxide emissions: 1850–2005, *Atmos. Chem. Phys.*, 11(3), 1101-1116, <https://doi.org/10.5194/acp-11-1101-2011>, 2011.

Song, F., Gao, Y.: Chemical characteristics of precipitation at metropolitan Newark in the US East Coast. *Atmos. Environ.* 43, 4903-4913, <https://doi.org/10.1016/j.atmosenv.2009.07.024>, 2009.

Song, H., K. Zhang, S. Piao, and S. Wan.: Spatial and temporal variations of spring dust emissions in northern China over the last 30 years, *Atmos. Environ.*, 126, 117-127, <https://doi.org/10.1016/j.atmosenv.2015.11.052>, 2016.

Song, Y., Y. Zhang, S. Xie, L. Zeng, M. Zheng, L. G. Salmon, M. Shao, and S. Slanina.: Source apportionment of PM_{2.5} in Beijing by positive matrix factorization, *Atmos. Environ.*, 40(8), 1526-1537, <https://doi.org/10.1016/j.atmosenv.2005.10.039>, 2006.

Sun, L., L. Li, Z. Chen, J. Wang, and Z. Xiong.: Combined effects of nitrogen deposition and biochar application on emissions of N₂O, CO₂ and NH₃ from agricultural and forest soils, *Soil Sci. Plant Nutr.*, 60(2), 254-265, 2014.

Sun, S.D., Jiang, W., Gao, W.D.: Vehicle emission trends and spatial distribution in Shandong province, China, from 2000 to 2014, *Atmos. Environ.*, 147, 190-199, <https://doi.org/10.1016/j.atmosenv.2016.09.065>, 2016.

Song, M.-L., Zhang, W., Wang, S.-H.: Inflection point of environmental Kuznets curve in Mainland China. *Energy Policy* 57, 14-20., 2013.

Song, L., Kuang, F.H., Skiba, U., Zhu, B., Liu, X.J., Levy, P., Dore, A., Fowler, D.: Bulk deposition of organic and inorganic nitrogen in southwest China from 2008 to 2013, *Environ. Pollut.*, 227, 157-166, <https://doi.org/10.1016/j.envpol.2017.04.031>, 2017.

Tai, A. P., L. J. Mickley, and D. J. Jacob.: Correlations between fine particulate matter (PM_{2.5}) and meteorological variables in the United States: Implications for the sensitivity of PM_{2.5} to climate change, *Atmos. Environ.*, 44(32), 3976-3984, <https://doi.org/10.1016/j.atmosenv.2010.06.060>, 2010.

Tao, J., L. Zhang, R. Zhang, Y. Wu, Z. Zhang, X. Zhang, Y. Tang, J. Cao, and Y. Zhang.: Uncertainty assessment of source attribution of PM_{2.5} and its water-soluble organic carbon content using different biomass burning tracers in positive matrix factorization analysis-A case study in Beijing, China, *Sci. Total Environ.*, 543, 326-335, <https://doi.org/10.1016/j.scitotenv.2015.11.057>, 2016.

Teinilä, K., A. Frey, R. Hillamo, H. C. Tülp, and R. Weller.: A study of the sea-salt chemistry using size-segregated aerosol measurements at coastal Antarctic station Neumayer, *Atmos. Environ.*, 96, 11-19, <https://doi.org/10.1016/j.atmosenv.2014.07.025>, 2014.

Teng, X., Q. Hu, L. Zhang, J. Qi, J. Shi, H. Xie, H. Gao, and X. Yao.: Identification of major sources of

atmospheric NH₃ in an urban environment in northern China during wintertime, *Environ. Sci. Technol.*, 51, 6839–6848, 10.1021/acs.est.7b00328, 2017.

Tian, H., J. Gao, L. Lu, D. Zhao, K. Cheng, and P. Qiu.: Temporal trends and spatial variation characteristics of hazardous air pollutant emission inventory from municipal solid waste incineration in China, *Environ. Sci. Technol.*, 46(18), 10364–10371, 10.1021/es302343s, 2012.

Tian, H., K. Liu, J. Hao, Y. Wang, J. Gao, P. Qiu, and C. Zhu.: Nitrogen oxides emissions from thermal power plants in China: Current status and future predictions, *Environ. Sci. Technol.*, 47(19), 11350–11357, 10.1021/es402202d, 2013.

Tian, H., K. Liu, J. Zhou, L. Lu, J. Hao, P. Qiu, J. Gao, C. Zhu, K. Wang, and S. Hua.: Atmospheric Emission Inventory of Hazardous Trace Elements from China's Coal-Fired Power Plants Temporal Trends and Spatial Variation Characteristics, *Environ. Sci. Technol.*, 48(6), 3575–3582, 10.1021/es404730j, 2014.

Turekian, K. K.: *Oceans*, Prentice-Hall, New Jersey, United States, 1968.

Tsai, Y.I., Hsieh, L.Y., Kuo, S.C., Chen, C.L., Wu, P.L.: Seasonal and rainfall-type variations in inorganic ions and dicarboxylic acids and acidity of wet deposition samples collected from subtropical East Asia. *Atmos. Environ.* 45, 3535–3547, <https://doi.org/10.1016/j.atmosenv.2011.04.001>, 2011.

Vašát, R., L. Pavlů, L. Borůvka, V. Tejnecký, and A. Nikodem.: Modelling the impact of acid deposition on forest soils in north Bohemian Mountains with two dynamic models: The Very Simple Dynamic Model (VSD) and the Model of Acidification of Groundwater in Catchments (MAGIC), *Soil Water Res.*, 10(1), 10–18, 2015.

Velthof, G., J. Lesschen, J. Webb, S. Pietrzak, Z. Miatkowski, M. Pinto, J. Kros, and O. Oenema.: The impact of the Nitrates Directive on nitrogen emissions from agriculture in the EU-27 during 2000–2008,

Sci. Total Environ., 468, 1225-1233, <https://doi.org/10.1016/j.scitotenv.2013.04.058>, 2014.

Wang, F.Y., Liu, R.J., Lin, X.G., Zhou, J.M.: Arbuscular mycorrhizal status of wild plants in saline-alkaline soils of the Yellow River Delta. *Mycorrhiza* 14, 133-137, 2004.

Wang, H., J. An, M. Cheng, L. Shen, B. Zhu, Y. Li, Y. Wang, Q. Duan, A. Sullivan, and L. Xia.: One year online measurements of water-soluble ions at the industrially polluted town of Nanjing, China: Sources, seasonal and diurnal variations, *Chemosphere*, 148, 526-536, <https://doi.org/10.1016/j.chemosphere.2016.01.066>, 2016a.

[Wang, J., Oiu, Y., He, S.T., Liu, N., Xiao, C.Y., Liu, L.X.: Investigating the driving forces of NOx generation from energy consumption in China. *Atmos. Chem. Physics*, 184, 836-846, 2018.](#)

Wang, K., H. Tian, S. Hua, C. Zhu, J. Gao, Y. Xue, J. Hao, Y. Wang, and J. Zhou.: A comprehensive emission inventory of multiple air pollutants from iron and steel industry in China: temporal trends and spatial variation characteristics, *Sci. Total Environ.*, 559, 7-14, <https://doi.org/10.1016/j.scitotenv.2016.03.125>, 2016b.

Wang, S., K. Luo, X. Wang, and Y. Sun (2016c), Estimate of sulfur, arsenic, mercury, fluorine emissions due to spontaneous combustion of coal gangue: An important part of Chinese emission inventories, *Environ. Pollut.*, 209, <https://doi.org/10.1016/j.envpol.2015.11.026>, 107-113.

Wang, Y., R. Wang, J. Ming, G. Liu, T. Chen, X. Liu, H. Liu, Y. Zhen, and G. Cheng (2016d), Effects of dust storm events on weekly clinic visits related to pulmonary tuberculosis disease in Minqin, China, *Atmos. Environ.*, 127, <https://doi.org/10.1016/j.atmosenv.2015.12.041>, 205-212.

Wang, Q.: Effects of urbanisation on energy consumption in China, *Energ. Policy*, 65, 332-339, 2014.

Wang, Q., G. Zhuang, K. Huang, T. Liu, C. Deng, J. Xu, Y. Lin, Z. Guo, Y. Chen, and Q. Fu.: Probing the severe haze pollution in three typical regions of China: Characteristics, sources and regional impacts,

Atmos. Environ., 120, 76-88, <https://doi.org/10.1016/j.atmosenv.2015.08.076>, 2015a.

Wang, X., W. Pu, J. Shi, J. Bi, T. Zhou, X. Zhang, and Y. Ren.: A comparison of the physical and optical properties of anthropogenic air pollutants and mineral dust over Northwest China, *Acta Meteorol Sin.*, 29(2), 180-200, 2015b.

Wang, Y., Y. Xue, H. Tian, J. Gao, Y. Chen, C. Zhu, H. Liu, K. Wang, S. Hua, and S. Liu.: Effectiveness of temporary control measures for lowering PM_{2.5} pollution in Beijing and the implications, *Atmos. Environ.*, 157, 75-83, <https://doi.org/10.1016/j.atmosenv.2017.03.017>, 2017.

Wei, F. S., Chen, J. S., Wu, Y. Y., Zheng, C.J.: The study of background value in soil across China. *Environ. Sci.*, 12, 12-20, 1991 (in Chinese).

Wei, F.S., Yang, G.Z., Jiang, D.Z., Liu, Z.H., Sun, B.M.: The basic statistics and characteristics of soil elements in China. *Environ. Moni. China.*, 7, 1-6, 1991 (in Chinese).

Wu, J., Li, P., Qian, H., Duan, Z., Zhang, X.: Using correlation and multivariate statistical analysis to identify hydrogeochemical processes affecting the major ion chemistry of waters: a case study in Laoheba phosphorite mine in Sichuan, China, *Arab. J. Geosci.*, 7, 3973–3982, 2014.

Wu, Q., and G. Han.: Sulfur isotope and chemical composition of the precipitation at the Three Gorges Reservoir, *Atmos. Res.*, 155, 130-140, <https://doi.org/10.1016/j.atmosres.2014.11.020>, 2015.

Wu, J., G. Liang, D. Hui, Q. Deng, X. Xiong, Q. Qiu, J. Liu, G. Chu, G. Zhou, and D. Zhang.: Prolonged acid rain facilitates soil organic carbon accumulation in a mature forest in Southern China, *Sci. Total Environ.*, 544, 94-102, <https://doi.org/10.1016/j.scitotenv.2015.11.025>, 2016a.

Wu, X.M., Wu, Y., Zhang, S.J., Liu, H., Fu, L.X., Hao, J.M.: Assessment of vehicle emission programs in China during 1998-2013: achievement, challenges and implications, *Environ. Pollut.*, 214, 556-567, <https://doi.org/10.1016/j.envpol.2016.04.042>, 2016b.

Xiao, H.W., H.-Y. Xiao, A.-M. Long, Y.-L. Wang, and C.-Q. Liu.: Sources and meteorological factors that control seasonal variation of $\delta^{34}\text{S}$ values in precipitation, *Atmos. Res.*, 149, 154-165, <https://doi.org/10.1016/j.atmosres.2014.06.003>, 2014.

Xing, J., J. Song, H. Yuan, X. Li, N. Li, L. Duan, X. Kang, and Q. Wang.: Fluxes, seasonal patterns and sources of various nutrient species (nitrogen, phosphorus and silicon) in atmospheric wet deposition and their ecological effects on Jiaozhou Bay, North China, *Sci. Total Environ.*, 576, 617-627, <https://doi.org/10.1016/j.scitotenv.2016.10.134>, 2017.

Xu, P., Y. Liao, Y. Lin, C. Zhao, C. Yan, M. Cao, G. Wang, and S. Luan.: High-resolution inventory of ammonia emissions from agricultural fertilizer in China from 1978 to 2008, *Atmos. Chem. Phys.*, 16(3), 1207-1218, <https://doi.org/10.5194/acp-16-1207-2016>, 2016.

Xu, W., X. Luo, Y. Pan, L. Zhang, A. Tang, J. Shen, Y. Zhang, K. Li, Q. Wu, and D. Yang.: Quantifying atmospheric nitrogen deposition through a nationwide monitoring network across China, *Atmos. Chem. Phys.*, 15(21), 12345-12360, <https://doi.org/10.5194/acp-15-12345-2015>, 2015.

Yan, W., E. Mayorga, X. Li, S. P. Seitzinger, and A. Bouwman.: Increasing anthropogenic nitrogen inputs and riverine DIN exports from the Changjiang River basin under changing human pressures, *Global Biogeochem. Cy.*, 24(4), <https://doi.org/10.1029/2009GB003575>, 2010.

Yang, K., J. Zhu, J. Gu, L. Yu, and Z. Wang.: Changes in soil phosphorus fractions after 9 years of continuous nitrogen addition in a *Larix gmelinii* plantation, *Ann. For. Sci.*, 72(4), 435-442, 2015.

Yang, X., Shen, S.H., Ying, F., He, Q., Ali, M., Huo, W., Liu, X.C.: Spatial and temporal variations of blowing dust events in the Taklimakan Desert, *Theor. Appl. Climato.*, 125, 669-677, 2016a.

Yang, Y., R. Zhou, Y. Yan, Y. Yu, J. Liu, Z. Du, and D. Wu.: Seasonal variations and size distributions of water-soluble ions of atmospheric particulate matter at Shigatse, Tibetan Plateau, *Chemosphere*, 145,

560-567, <https://doi.org/10.1016/j.chemosphere.2015.11.065>, 2016b.

Yang, X., S. Wang, W. Zhang, and J. Yu.: Are the temporal variation and spatial variation of ambient SO₂ concentrations determined by different factors? *J. Clean Prod.*, 167, 824-836, <https://doi.org/10.1016/j.jclepro.2017.08.215>, 2017.

Yu, H. L., He, N. P., Wang, Q. F., Zhu, J. X., Xu, L., Zhu, Z. L., Yu, G. R.: Wet acid deposition in Chinese natural and agricultural ecosystems: Evidence from national-scale monitoring, *J. Geophys. Res. Atmos.*, 121, 1-11, <https://doi.org/10.1002/2015JD024441>, 2016.

Yu, H., N. He, Q. Wang, J. Zhu, Y. Gao, Y. Zhang, Y. Jia, and G. Yu.: Development of atmospheric acid deposition in China from the 1990s to the 2010s, *Environ. Pollut.*, 231, 182-190, <https://doi.org/10.1016/j.envpol.2017.08.014>, 2017a.

Yu, Y., S. Zhao, B. Wang, P. Fu, and J. He.: Pollution Characteristics Revealed by Size Distribution Properties of Aerosol Particles at Urban and Suburban Sites, Northwest China, *Aerosol Air Qual Re.*, 17(7), 1784-1797, 10.4209/aaqr.2016.07.0330, 2017b.

Zhai, P.M., Li, X.Y.: On climate background of duststorms over northern China, *Acta Geographica Sinica*, 58, 2003 (in Chinese).

[Zhan, Y., Luo, Y.Z., Deng, X.F., Zhang, K.S., Zhang, M.H., Grieneisen, M.L., Di, B.F., 2018. Satellited-based estimates of daily NO₂ exposure in China using hybrid random forest and spatiotemporal Kriging model. *Environ. Sci. Tech.* 52, 4180-4189, 2018.](#)

Zhang, S.L., Yang, G.Y.: Changes of background values of inorganic elements in soils of gunagdong province, *Soils*, 1009-1014, 2012 (in Chinese).

Zhang, T., J. Cao, X. Tie, Z. Shen, S. Liu, H. Ding, Y. Han, G. Wang, K. Ho, and J. Qiang.: Water-soluble ions in atmospheric aerosols measured in Xi'an, China: seasonal variations and sources, *Atmos Res.*,

带格式的: 下标

102(1), 110-119, <https://doi.org/10.1016/j.atmosres.2011.06.014>, 2011.

Zhang, X.-X., B. Sharratt, X. Chen, Z.-F. Wang, L.-Y. Liu, Y.-H. Guo, J. Li, H.-S. Chen, and W.-Y. Yang.: Dust deposition and ambient PM₁₀ concentration in northwest China: spatial and temporal variability, *Atmos. Chem. Phys.*, 17(3), 1699-1711, <https://doi.org/10.5194/acp-17-1699-2017>, 2017a.

Zhang, Y., J. Wei, A. Tang, A. Zheng, Z. Shao, and X. Liu.: Chemical Characteristics of PM_{2.5} during 2015 Spring Festival in Beijing, China, *Aerosol Air Qual. Re.*, 17(5), 1169-1180, 10.4209/aaqr.2016.08.0338, 2017b.

Zhang, Z., J. Gao, L. Zhang, H. Wang, J. Tao, X. Qiu, F. Chai, Y. Li, and S. Wang.: Observations of biomass burning tracers in PM_{2.5} at two megacities in North China during 2014 APEC summit, *Atmos. Environ.*, 169, 54-64, <https://doi.org/10.1016/j.atmosenv.2017.09.011>, 2017c.

Zhang, X., F. Chai, S. Wang, X. Sun, and M. Han.: Research progress of acid precipitation in China, *Res. Environ. Sci.*, 23(5), 527-532, 2010 (in Chinese).

Zhang, Y.Y., Liu, J.F., Mu, Y.J., Pei, S.W., Lun, X.X., Chai, F.H.: Emissions of nitrous oxide, nitrogen oxides and ammonia from a maize field in the North China Plain, *Atmos. Environ.*, 45, 2956-2961, <https://doi.org/10.1016/j.atmosenv.2010.10.052>, 2011.

Zhang, Y., W. Huang, T. Cai, D. Fang, Y. Wang, J. Song, M. Hu, and Y. Zhang.: Concentrations and chemical compositions of fine particles (PM_{2.5}) during haze and non-haze days in Beijing, *Atmos. Res.*, 174, 62-69, <https://doi.org/10.1016/j.atmosres.2016.02.003>, 2016.

Zhao, C., and K. Luo.: Sulfur, arsenic, fluorine and mercury emissions resulting from coal-washing byproducts: A critical component of China's emission inventory, *Atmos. Environ.*, 152, 270-278, <https://doi.org/10.1016/j.atmosenv.2016.12.001>, 2017.

Zhao, J., F. Zhang, Y. Xu, and J. Chen.: Characterization of water-soluble inorganic ions in size-

segregated aerosols in coastal city, Xiamen, Atmos. Res., 99(3), 546-562, <https://doi.org/10.1016/j.atmosres.2010.12.017>, 2011.

Zhao, M., S. Wang, J. Tan, Y. Hua, D. Wu, and J. Hao.: Variation of urban atmospheric ammonia pollution and its relation with PM_{2.5} chemical property in winter of Beijing, China, Aerosol Air Qual. Res., 16(6), 1378-1389, 10.4209/aaqr.2015.12.0699, 2016.

Zheng, B., H. Huo, Q. Zhang, Z. Yao, X. Wang, X. Yang, H. Liu, and K. He.: High-resolution mapping of vehicle emissions in China in 2008, Atmos. Chem. Phys., 9787, <https://doi.org/10.5194/acp-14-9787-2014>, 2014.

Zhou, Y., Y. Zhao, P. Mao, Q. Zhang, J. Zhang, L. Qiu, and Y. Yang.: Development of a high-resolution emission inventory and its evaluation and application through air quality modeling for Jiangsu Province, China, Atmos. Chem. Phys., 17(1), 211-233, <https://doi.org/10.5194/acp-17-211-2017>, 2017a.

Zhou, Y., Xing, X.F., Lang, J.L., Chen, D.S., Cheng, S.Y., Wei, L., Wei, X., Liu, C.: A comprehensive biomass burning emission inventory with highspatial and temporal resolution in China, Atmos. Chem. Phys., 17, 2839-2864, <https://doi.org/10.5194/acp-17-2839-2017>, 2017b.

Figure and table caption

- Fig. 1** The spatial distribution of 320 cities and five ecological regions.
- Fig. 2** The inter-annual and seasonal variation of pH and EC of the precipitation in China.
- Fig. 3** The spatial distribution of pH and EC of the precipitation in China.
- Fig. 4** The temporal variation of water-soluble ions in the precipitation.
- Fig. 5** The spatial variation of NO_3^- , NH_4^+ , and SO_4^{2-} in the precipitation.
- Fig. 6** The spatial distribution of Ca^{2+} , Cl^- , F^- , K^+ , Mg^{2+} , and Na^+ in the precipitation.
- Fig. 7** The triangular diagrams of NF for main alkaline ions.
- Fig. 8** The EF_{sea} and EF_{soil} of NO_3^- , SO_4^{2-} , and NH_4^+ .
- Fig. 9** The spatial variation of SSF, CF, and AF for NO_3^- , NH_4^+ , and SO_4^{2-} in the precipitation.
- Fig. 10** The seasonal difference of contribution ratios of anthropogenic source, crustal source, and sea source.
- Fig. 11** The local regression coefficient of influential factors for the NO_3^- , NH_4^+ , and SO_4^{2-} .
- Tab. 1** The comparison of physicochemical properties and chemical composition in the precipitation.
- Tab. 2** The mean enrichment factor relative to sea and soil, and the source contribution (%) of major ions in China (SSF denotes sea salt fraction, CF represents the crustal source, AF indicates the anthropogenic fraction).
- Tab. 3** The loading matrix of precipitation in four seasons of China.
- Tab. 4** The results of stepwise regression method.

Fig. 1

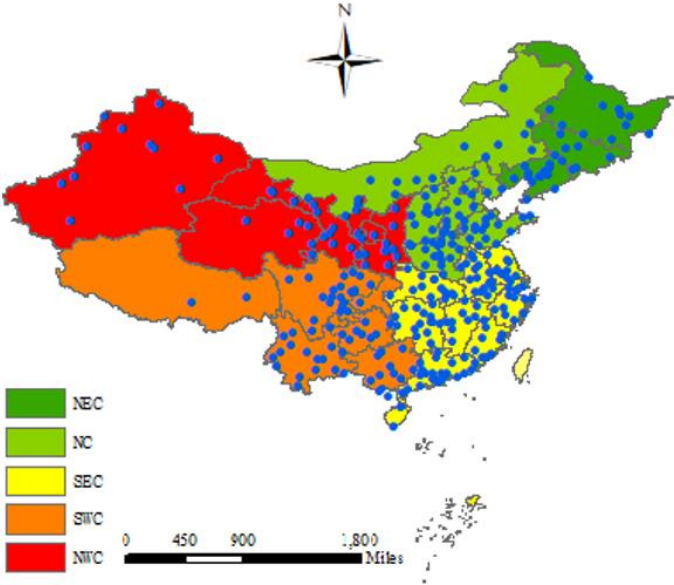


Fig. 2

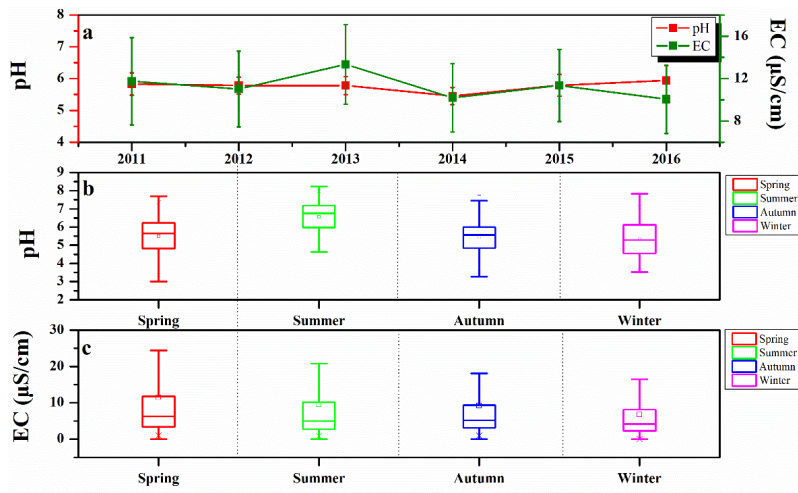


Fig. 3

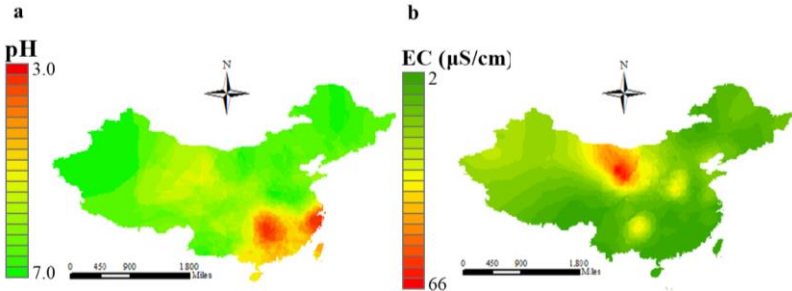


Fig. 4

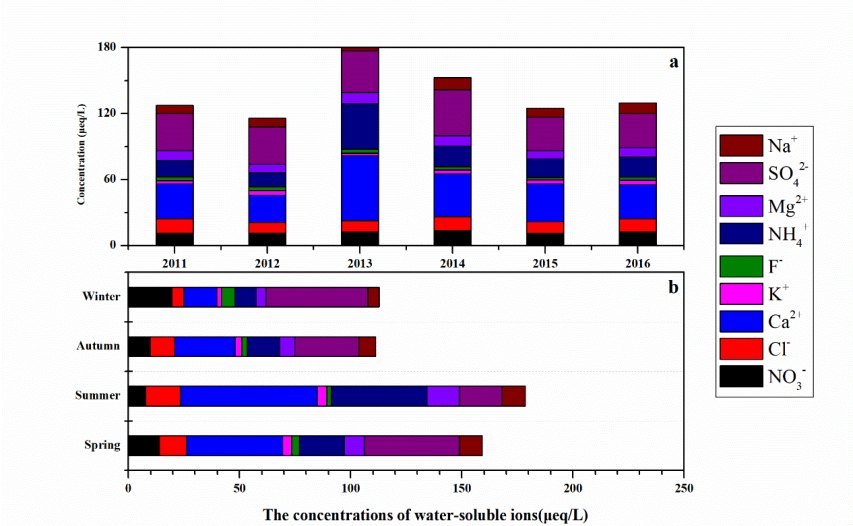


Fig. 5

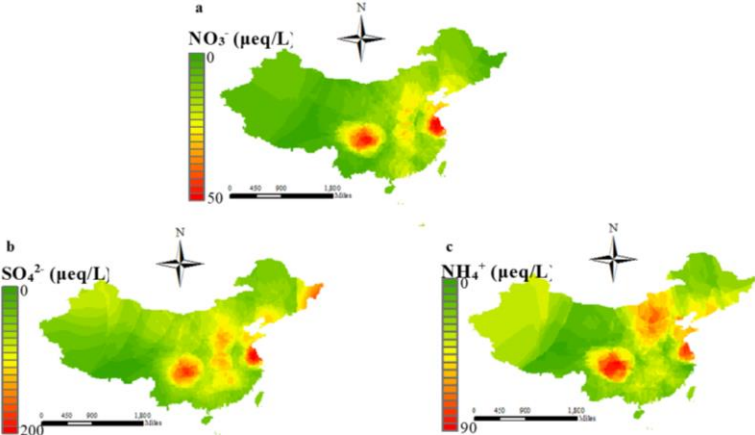


Fig. 6

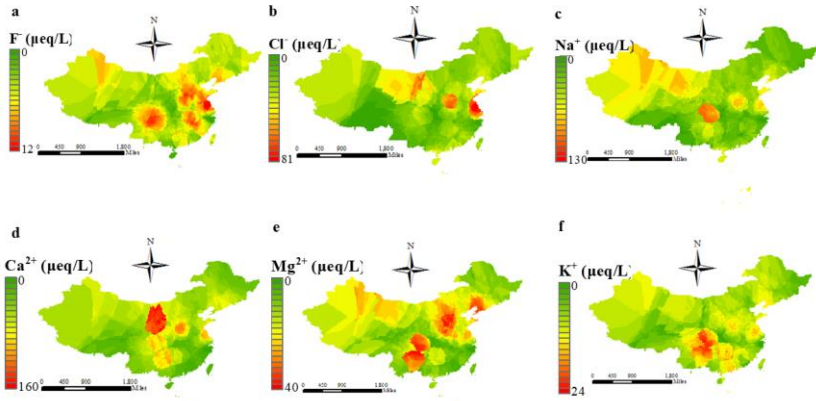


Fig. 7

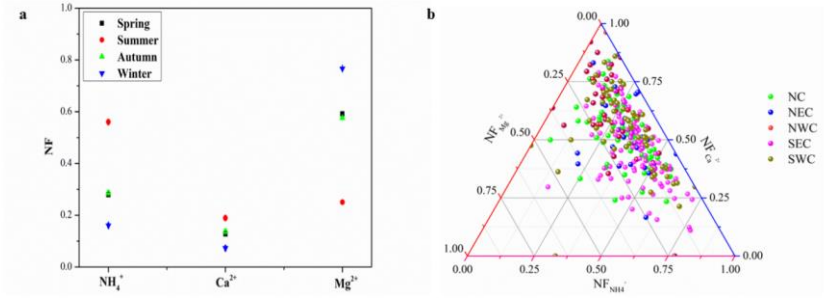


Fig. 8

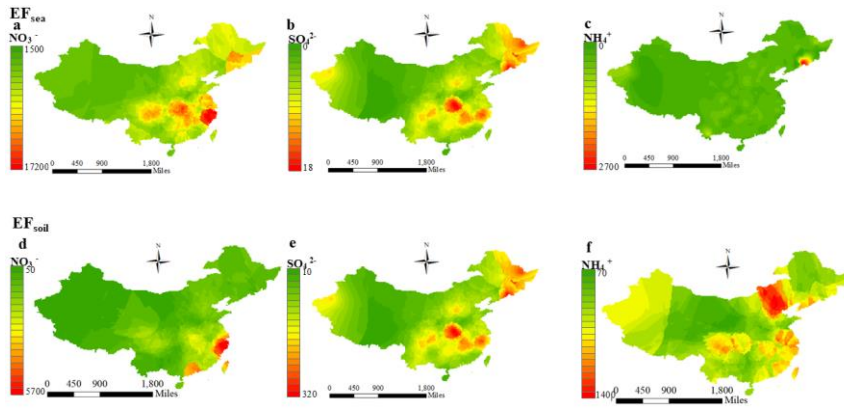


Fig. 9

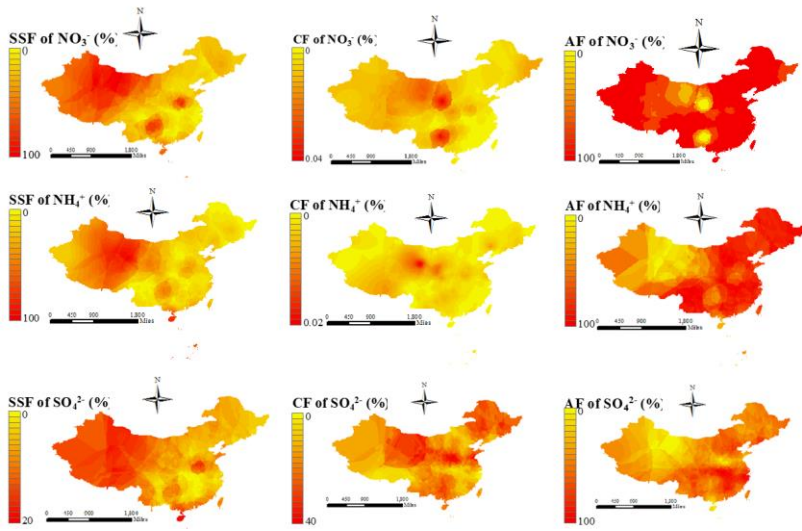


Fig. 10

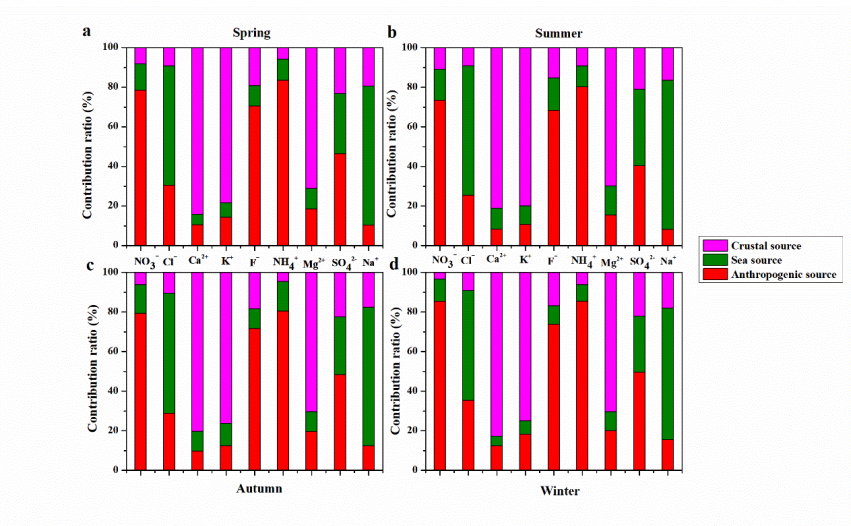
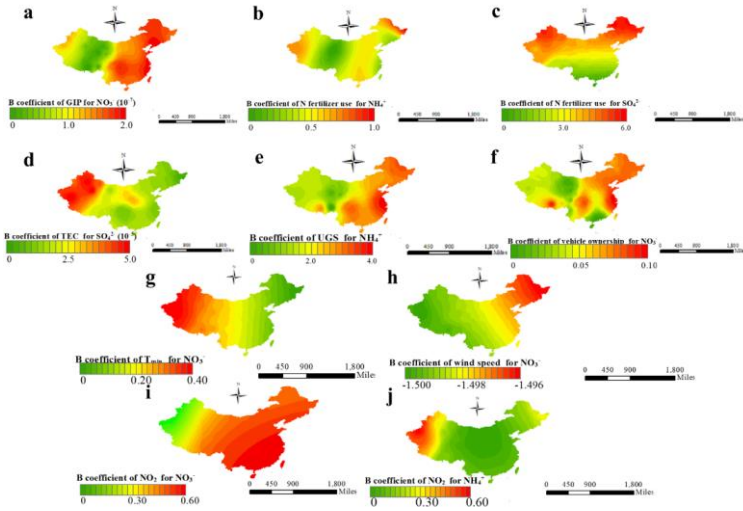


Fig. 11



Tab. 1

	pH	EC	NO ₃ ⁻	Cl ⁻	Ca ²⁺	K ⁺	F ⁻	NH ₄ ⁺	Mg ²⁺	SO ₄ ²⁻	Na ⁺	Year	References
Beijing	5.68	9.89	15.13	6.62	26.27	1.80	2.24	45.33	5.51	31.28	3.39	2011-	This study
Zhengzhou	6.09	26.44	37.10	72.45	109.23	8.25	5.80	23.82	20.54	25.80	6.40	2011-	This study
Harbin	6.13	7.41	9.87	20.71	21.98	5.02	5.03	11.96	9.55	28.76	22.00	2011-	This study
Shenyang	5.76	8.40	24.52	15.90	75.32	2.59	4.32	40.68	22.68	57.57	16.88	2011-	This study
Qingdao	5.32	16.53	5.25	5.79	28.18	2.07	1.34	9.28	9.80	10.96	25.30	2011-	This study
Shanghai	4.39	2.50	40.06	4.15	19.09	1.07	1.45	17.48	4.71	29.13	20.36	2011-	This study
Wuhan	4.68	2.66	11.61	2.12	13.55	0.76	1.07	9.38	2.63	27.93	1.28	2011-	This study
Guangzhou	4.98	2.84	26.74	19.38	41.60	9.42	3.93	13.58	8.33	35.76	9.57	2011-	This study
Chengdu	4.89	6.03	48.08	22.13	44.42	12.60	9.21	65.19	8.23	77.16	15.06	2011-	This study
Lhasa	5.21	4.51	0.50	1.65	7.66	0.48	0.94	0.91	1.28	1.44	1.62	2011-	This study
Urumqi	6.13	13.41	16.87	30.38	115.24	4.76	2.02	73.76	19.41	56.76	28.87	2011-	This study
Lanzhou	5.05	58.06	16.19	4.93	51.84	1.24	1.57	3.05	8.17	33.30	10.87	2011-	This study
Jiuzhaigou	5.95	15.70	9.10	44.10	55.80	34.80	0.86	18.40	5.60	15.90	12.60	2015-	Qiao et al. (2018)
Yulong	5.94	10.30	4.00	1.96	37.7	2.46	1.20	13.20	5.68	28.30	3.72	2012	Niu et al. (2014)
Nam Co	6.59	19.70	10.00	19.20	301	14.50	-	18.10	7.43	15.50	15.40	2005	Li et al. (2007)
Southern	-	-	20.97	31.06	46.68	11.14	-	58.57	22.55	45.97	56.41	2005-	Tsai et al. (2011)
Petra,	6.80	160	35.70	80.60	163.10	26.30	-	18.40	62.30	53.20	75.60	2002-	Al-Khashman et al. (2005)
Tokyo,	4.52	-	30.50	55.20	24.90	2.90	-	40.4	11.5	50.2	37.0	1990-	Okuda et al. (2005)
Guaiba,	5.92	10.8	4.00	13.80	21.50	5.81	5.90	38.90	8.85	23.10	15.10	2002	Migliavacca et al. (2005)
Sao Paulo,	-	-	15.60	0.90	5.50	3.70	-	27.90	1.70	8.60	3.60	2000	Fornaro and Gutz (2003).
Singapore	-	-	16.80	22.10	21.7	3.96	-	17.3	7.46	58.7	31.1	1997-	Balasubramanian et al. (2001)
Newark,	-	-	14.40	10.70	6.00	1.30	-	24.40	3.30	38.10	10.90	2006-	Song and Gao (2009)
Patras,	5.16	--	19.40	114.30	98.50	6.60	--	16.30	30.40	46.10	90.20	2000-	Glavas and Moschonas (2002)
Sardinia,	5.18	--	29	322	70	17	--	25	77	90	252	1992-	Le Bolloch and Guerzoni (1995)
Adirondack,	4.50	--	22.60	2.14	3.59	0.33	--	10.50	0.99	36.90	1.61	1988-	Ito et al. (2002)

Tab. 2

	EF _{sea}	EF _{soil}	SSF	CF	AF
NO ₃ ⁻	3507.49	59.36	0	0.02	99.98
Cl ⁻	1.13	169.88	88.31	0.59	11.10
Ca ²⁺	231.56	1.00	0.06	99.94	0
K ⁺	16.16	0.83	4.88	95.12	0
F ⁻	5864.28	9.96	0.02	10.04	89.94
NH ₄ ⁺	10.51	86.31	0.10	0.01	99.89
Mg ²⁺	10.18	0.55	2.94	97.06	0
SO ₄ ²⁻	7.22	5.13	13.85	19.50	66.65
Na ⁺	1.00	1.83	64.66	35.34	0

Tab. 3

Season	Variable	F1	F2	F3
Overall	NO ₃ ⁻	0.71	0.24	0.45
	Cl ⁻	0.43	0.64	-0.12
	Ca ²⁺	0.42	-0.22	0.75
	K ⁺	0.39	0.18	0.72
	F ⁻	0.68	-0.20	0.45
	NH ₄ ⁺	0.74	0.35	0.13
	Mg ²⁺	-0.41	0.10	0.66
	SO ₄ ²⁻	0.63	0.23	0.14
	Na ⁺	-0.02	0.65	0.45
Spring	NO ₃ ⁻	0.76	0.11	-0.32
	Cl ⁻	-0.33	0.59	0.26
	Ca ²⁺	0.32	-0.16	0.80
	K ⁺	-0.36	0.06	0.78
	F ⁻	0.70	-0.10	0.20
	NH ₄ ⁺	0.68	0.29	-0.46
	Mg ²⁺	-0.38	0.42	0.69
	SO ₄ ²⁻	0.77	0.31	0.22
	Na ⁺	-0.04	0.72	0.46
Summer	NO ₃ ⁻	0.63	0.24	-0.33
	Cl ⁻	0.42	0.66	-0.38
	Ca ²⁺	0.44	-0.26	0.85
	K ⁺	-0.37	0.19	0.70
	F ⁻	0.54	-0.32	0.48
	NH ₄ ⁺	0.59	0.33	-0.47
	Mg ²⁺	0.32	-0.38	0.60
	SO ₄ ²⁻	0.56	0.36	0.34
	Na ⁺	-0.09	0.75	0.49
Autumn	NO ₃ ⁻	0.73	-0.14	0.38
	Cl ⁻	-0.39	0.62	0.29
	Ca ²⁺	0.32	-0.16	0.80
	K ⁺	0.45	-0.09	0.68
	F ⁻	0.68	-0.15	0.28

	NH ₄ ⁺	0.69	0.42	-0.45
	Mg ²⁺	-0.29	0.32	0.71
	SO ₄ ²⁻	0.68	-0.29	0.23
	Na ⁺	-0.14	0.69	-0.37
Winter	NO ₃ ⁻	0.79	0.23	-0.36
	Cl ⁻	-0.38	0.49	0.29
	Ca ²⁺	0.39	-0.35	0.65
	K ⁺	-0.39	0.08	0.72
	F ⁻	0.75	0.08	-0.24
	NH ₄ ⁺	0.73	0.26	-0.42
	Mg ²⁺	0.35	-0.49	0.75
	SO ₄ ²⁻	0.79	0.22	0.36
	Na ⁺	-0.16	0.54	0.33

Tab. 4

Dependent variables	Independent variables	Partial regression coefficients	R ²	t value	p value
NO ₃ ⁻	GIP	8.42×10 ⁻⁸	0.62	4.03	0.00
	Vehicle ownership	0.03		-2.39	0.01
	NO ₂	0.34		4.29	0.00
	T _{min}	0.15		1.34	0.02
	Wind speed	-1.49		-1.69	0.03
Cl ⁻	Dust days	0.12	0.52	2.14	0.04
Ca ²⁺	PM ₁₀	0.36	0.56	3.26	0.00
	Dust days	132.74		2.99	0.00
K ⁺	Dust days	2.09	0.49	2.03	0.02
F ⁻	GIP	0.54×10 ⁻⁷	0.50	2.31	0.02
NH ₄ ⁺	N fertilizer use	0.14	0.48	2.46	0.02
	UGS	1.33×10 ⁻⁴		1.79	0.04
	NO ₂	0.25		1.98	0.03
Mg ²⁺	Dust days	2.36	0.43	1.65	0.05
SO ₄ ²⁻	TEC	2.80×10 ⁻⁵	0.64	3.07	0.00
	N fertilizer use	3.36		3.59	0.00
Na ⁺	Dust days	2.46	0.46	1.69	0.04